Synthesis and Characterization of Nanofluid for Heat Transfer Application

By

Muhammad Assad Khan

00000205578

Session 2017-19

Supervision of

Dr. Majid Ali

A Thesis Submitted to U.S. – Pak Centers for Advance Studies in Energy in partial fulfillment of the requirements for the degree of Master of Science in

THERMAL ENERGY ENGINEERING

U.S. – Pak Centers for Advance Studies in Energy (USPCAS-E)

National University of Sciences and Technology (NUST)

H-12, Islamabad 44000, Pakistan

2020

Synthesis and Characterization of Nanofluid for Heat Transfer Application

By

Muhammad Assad Khan

00000205578

Session 2017-19

Supervision of

Dr. Majid Ali

A Thesis Submitted to U.S. – Pak Centers for Advance Studies in Energy in partial fulfillment of the requirements for the degree of Master of Science in

THERMAL ENERGY ENGINEERING

U.S. – Pak Centers for Advance Studies in Energy (USPCAS-E)

National University of Sciences and Technology (NUST)

H-12, Islamabad 44000, Pakistan

2020

THESIS ACCEPTANCE CERTIFICATE

This is certified that final copy of MS/MPhil thesis written by Mr. Muhammad Assad Khan, (Registration No. 00000205578), of U.S.-Pak Centers for Advance Studies in Energy has been vetted by undersigned, found complete in all respects as per NUST Statues/Regulations, is within similarities indices limit and accepted as partial fulfillment for award of MS/MPhil degree. It is further certified that necessary amendments as pointed out by GEC members of the scholar have also been incorporated in the said thesis.

Signature: _____

Supervisor Dr. Majid Ali

Date: _____

Signature: _____

HoD-TEE Dr. Adeel Javed

Date: _____

Signature: _____

A/Principal Dr. Adeel Waqas

Date: _____

Certificate

This is to certify that work in this thesis has been carried out by **Mr. Muhammad Assad Khan** and completed under my supervision in, U.S.-Pak Centers for Advance Studies in Energy, National University of Sciences and Technology, H-12, Islamabad, Pakistan.

Supervisor: _____

Dr. Majid Ali
U.S.-Pak Centers for Advance Studies in Energy
NUST, Islamabad

GEC member 1: _____

Dr. Adeel Waqas
U.S.-Pak Centers for Advance Studies in Energy
NUST, Islamabad

GEC member 2: _____

Dr. Nadia Shahzad
U.S.-Pak Centers for Advance Studies in Energy
NUST, Islamabad

GEC member 3: _____

Dr. Naseem Iqbal
U.S.-Pak Centers for Advance Studies in Energy
NUST, Islamabad

HoD-TEE: _____

Dr. Adeel Javed
U.S.-Pak Centers for Advance Studies in Energy
NUST, Islamabad

A/Principal: _____

Dr. Adeel Waqas
U.S.-Pak Centers for Advance Studies in Energy
NUST, Islamabad

Acknowledgments

I am extremely thankful to Allah Almighty without whose help I would not have been able to complete this work. All the help and support from my parents and teachers were only because of Allah's Will.

I am thankful to my supervisor, Dr. Majid Ali, for the tremendous supervision, motivation, and guidance he has conveyed throughout my time as his understudy. I have been exceptionally honored to have a supervisor who thought such a great amount about my work, and who responded to my inquiries and questions immediately.

I am thankful to Principal Dr. Adeel Waqas, HoD TEE Dr. Adeel Javed, lab engineers, lab technicians, all GEC members, USPCAS-E and USAID for their provision all over the program.

I am especially appreciative of my parents who supported me throughout my life.

Thank you

Muhammad Assad Khan

I dedicate this thesis to my family, who always supported me and taught me how to fight against the struggles of life, my father who supported me through every thick and thin of life, my mother who taught me to be patient and work hard until you achieve your goals, my teachers whom guidance helped me to achieve this status in my life.

Abstract

Nanofluid is nanomaterials suspension in the base fluid. It possesses better thermal properties and has better potential for heat transport in different applications compared to conventional fluids, but the major concern is nanofluid stability and durability. In this study, nanofluid stability and thermal properties are evaluated for practical application. Titanium dioxide nanoparticles were synthesized using a chemical method and were characterized by scanning electron microscopy, energy dispersion X-ray spectroscopy and X-ray diffraction. Nanofluid was prepared using titanium dioxide particles and water by two steps method. Cetyl trimethyl ammonium bromide (CTAB) surfactant and probe ultrasonication were used to improve the stability of the nanofluid. sedimentation photo capturing and UV-Vis spectrophotometer was used for stability evaluation. Nanofluid viscosity was measured with viscometer and its variation was evaluated at different concentrations of the nanoparticles (0.05vol%, 0.1vol%, and 0.2 vol%) and temperatures (30 ^{o}C to 80 ^{o}C). This study further evaluates the variation of viscosity with shear rate (50 s^{-1} to 244 s^{-1}) applied to the sample. The formation of the spherical shape and anatase phase along with small amount of rutile phase of titanium dioxide nanoparticles are confirmed by experimental results. The stability of the nanofluid was observed to be enhanced significantly by the addition of surfactants. The viscosity of the nanofluid was found to have a direct relation with particle loading and shear rate while it has an inverse relation with the temperature of the sample. The thermal conductivity was observed to have direct relation with the amount of particle loadings in the nanofluid.

Contents

Abstract vi
List of Figures x
List of Publications xii
List of Abbreviations xiii
Chapter 1 1
Introduction 1
1.1 Development of Nanofluid 1
1.2 Nanoparticles 3
1.3 Nanofluid 3
1.4 Advantages of titanium dioxide nanofluid 4
1.5 Scope of study 4
1.6 Research Statement 5
1.7 Objectives 5
1.8 Organization of Thesis 5
Chapter 2 10
Literature Review 10
2.1 Preparation of the nanoparticles 10
2.2 Parameters affecting the shape, size, and phase of the particles 10
2.2.1 pH value 11
2.2.2 Calcination temperature 11
2.3 Nanofluid fabrication 11
2.3.1 One/single Step Method 11
2.3.2 Two-step method 11
2.4 Parameters affecting nanofluids stability 12
2.4.1 Ultrasonic vibration 12
2.4.2 Surfactants 12
2.4.3 pH value 13
2.4.4 Combination of processes 13
2.5 Stability measurement techniques for nanofluids 13
2.5.1 Spectral absorbency 14
2.5.2 Zeta potential analysis 14
2.5.3 Sedimentation photo capturing method 15
2.6 Viscosity 15
2.7 Parameters affecting the viscosity of the nanofluid 15

2.7.1 Particle loading....16
2.7.2 Temperature of nanofluid....16
2.7.3 Particle size and shape....17
2.7.4 Shear rate....17
2.7.5 Surfactants....17
2.7.6 Base fluid....18
2.8 Thermal conductivity....18
2.9 Parameters affecting thermal conductivity....19
2.9.1 Particle concentration....19
2.9.2 Temperature....20
2.9.3 Base fluid....21
2.9.4 Particle size....21
2.9.5 Particle shape....22
Chapter 3....29
Methodology....29
Chapter 4....32
Preparation and Characterization....32
4.1 Preparation of nanoparticles....32
4.2 Characterization....33
4.2.1 X-ray diffraction....33
4.2.2 Scanning Electron Microscopy (SEM) and Energy Dispersive X-ray spectroscopy (EDS)....34
4.3 Surfactants....36
4.4 Preparation of nanofluid....36
4.5 Ultrasound probe sonicator....37
4.6 Stability....38
4.6.1 UV-Vis Spectroscopy....38
4.6.2 Sedimentation Photo capturing....40
4.7 Thermo-physical properties of the nanofluid....40
4.7.1 Viscosity of the nanofluid....40
4.7.2 Thermal Conductivity....41
Chapter 5....45
Results and Discussions....45
5.1 Characterization of nanoparticles....45
5.1.1 X-Ray diffraction....45

5.1.2 Scanning Electron Microscopy 46
5.1.3 Energy-dispersive X-ray spectroscopy (EDS) 47
5.2 Stability evaluation of the nanofluid 47
5.2.1 UV-Vis spectroscopy 48
5.2.2 Sedimentation Photo capturing 49
5.3 Viscosity of nanofluid 51
5.4 Thermal conductivity of nanofluid 52
Chapter 6 59
Conclusion and Recommendations 59
Chapter 7 61
7.1 Introduction 61
7.2 Synthesis of NIPAM hydrogels 62
7.3 Swelling Test of NIPAM 62
7.4 lower critical solution temperature 63
7.5 Desalination using hydrogels 64

List of Figures

Figure 1.1 Application of nanofluid....2
Figure 1.2 methods for the preparation of nanoparticles....3
Figure 1.3 nanoparticles and nanofluids in literature....4
Figure 2.1 Thermal conductivity of different materials....19
Figure 3.1 Flow diagram of research work....30
Figure 4.1 Nanoparticles preparation process....33
Figure 4.2 Bruker D8 advanced X-ray diffractometer....34
Figure 4.3 TESAN VEGA3 Scanning electron microscope....36
Figure 4.4 Nanofluid fabrication process....37
Figure 4.5 QSonica Probe Sonicator....38
Figure 4.6 Block diagram of UV-Vis spectroscopy....39
Figure 4.7 T92+ UV-Vis spectrophotometer....40
Figure 4.8 Brookfield Viscometer DV2T....41
Figure 4.9 Thermal conductivity meter (Hot Disk TPS 2500s)....42
Figure 5.1 XRD Pattern of titanium dioxide nanoparticles....46
Figure 5.2 SEM image of titanium dioxide nanoparticles....47
Figure 5.3 EDS pattern of nanoparticles....47
Figure 5.4 UV-Vis spectra of 0.05vol% TiO_2- H_2O nanofluid without surfactant....48
Figure 5.5 UV-Vis spectra of 0.2vol% TiO_2- H_2O nanofluid with CTAB surfactant .49
Figure 5.6 Sedimentation photograph of 0.05vol% TiO_2- H_2O of nanofluid without surfactant (a) Before sonication (b) Day1 after sonication (c) Day17 (d) Day 32 (e) Day44 (f) Day 60 50
Figure 5.7 Sedimentation photograph of 0.2vol% TiO_2- H_2O of nanofluid with surfactant (a) Before sonication (b) Day1 after sonication (c) Day17 (d) Day 32 (e) Day44 (f) Day 60 50
Figure 5.8 Viscosity variation with temperature....51
Figure 5.9 Viscosity variation with shear rate 52
Figure 5.10 Viscosity variation with the concentration of nanoparticles 52
Figure 5.11 Thermal conductivity variation with Concentration of nanoparticles....54
Figure 5.12 Thermal conductivity enhancement 55
Figure 7.1 Hydrogels Desalination process……..62
Figure 7.2 Experimental setup for preparation of hydrogels……62
Figure 7.3 Swelling ratio against time NIPAM synthesized in inert and regular atmosphere……63
Figure 7.4 Experimental setup for determination of LCST……..63
Figure 7.5 LCST result of NIPAM……...64
Figure 7.6 (a) Dry hydrogel before absorbing water (b) hydrogel swells up after absorbing water……64
Figure 7.7 Permeation flux over 4 hour period in current study……..65
Figure 7.8 Permeation flux over 4 hour period comparison with Razmjou et al…….65

List of Tables

Table 5.1 Summary of thermal conductivity enhancement in different studies ..53
Table 5.2 Models used for predicting thermal conductivity of nanofluid 54

List of Publications

"Evaluation of Stability and Rheological Behavior of TiO_2-H_2O Nanofluid" presented at international conference of Mechanical engineering (ICME 2020) held at UET Lahore, Pakistan.

List of Abbreviations

TiO_2	Titanium dioxide
TTIP	Titanium tetra isopropoxide
CTAB	Cetyl tri-methyl ammonium bromide
XRD	X-Ray Diffraction
SEM	Scanning electron microscopy
UV-Vis	Ultra-violet Visible spectroscopy
wt. %	weight percentage
vol%	volume percentage

Chapter 1

Introduction

1.1 Development of Nanofluid

Nanofluid has better heat transfer capability because of improved thermal properties than conventional fluids which makes it a potential application in different industrial processes[1][2]. The potential area includes Automobile engine cooling[3]–[6], electronic devices cooling[7][8], solar heating Thermal transport [9]–[11], manufacturing industry,etc. In recent past researchers and scientists have worked hard in improving the performance of conventional fluid (ethylene glycol, water, and engine oil,etc.). The main difficulty faced was the poor ability of these conventional fluids to transport heat which restricted their use in industries. It is well known that metals have improved heat transport properties than fluids. It is found that copper has a thermal conductivity which is about 700 times the thermal conductivity of water and about 3000 times the thermal conductivity of engine oil thus it was expected that the fluids containing metal will definitely possess enhanced thermal conductivity as compared to conventional fluids [9]. In past people have tried to add millimeter size or micrometer size metals to the fluid to improve its heat transfer properties but the problems faced were aggregation, sedimentation, poor dispensability and adhering to the walls of system which can result in lowering heat transfer rate, increasing pump power requirement and may cause blocking pipes. Choi in 1995 at Argonne National laboratory USA discovered a revolutionary fluid known as nanofluid. The nanofluid discovered was the suspension of nanomaterial (nanoparticles, nanofibers, nanotubes, nanowires, nanorods and nanosheets) in conventional base fluid. The ability of fluid to carry more heat with less temperature difference results in better efficiency and better heat transfer performance. The nanofluid had better thermal properties and can carry more heat which shows better promise to be applied in various applications [12].

Nanofluid has various practical applications. One potential application is the automobile industry. We are aware of the increasing prices of petroleum and the need to develop more efficient systems. Scientists have tried to enhance the performance of an automobile cooling system and lower its size to decrease the weight load of the cooling system which will result in fuel-saving [13]. The cooling system performance can be improved either by improving the heat transfer performance of the coolant, by spot cooling or by increasing the surface area of the cooling system by using fins, etc. The higher surface area will result in increasing the weight load of the cooling system which can result in increasing the load on the engine and hence will need more fuel consumption, so the use of efficient coolant with better thermo-physical properties is a better option. Nanofluid has better thermo-physical properties and has shown better promise to be used for cooling purposes. Tribology study shows that the use of nanoparticles with the lubricating oil improves its performance in load carry, anti-wear characteristic and friction reduction[14]. The Solar collector is another application where nanofluid is can as absorbing medium or heat transfer medium in place of the base fluid and because of better heat transfer properties, nanofluid can result in better and efficient performance of the solar collector[9]. Electronic devices cooling is also one of the potential applications of the nanofluid where conventional fluids are used for cooling. If the conventional fluid is replaced with nanofluid it will result in better coolant performance and hence improved the performance of the cooling system because of the better properties of the nanofluid.

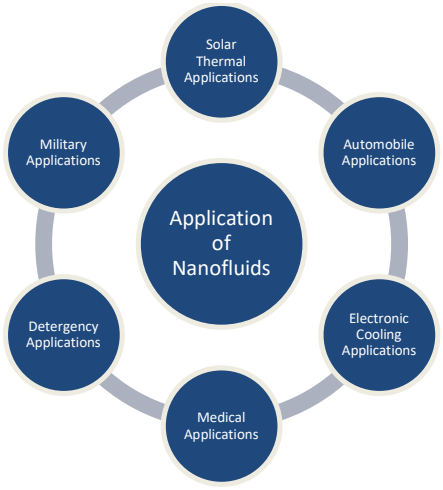

Figure 1.1 Application of nanofluid [2]

1.2 Nanoparticles

Particles or materials having nanometer size are referred to as nanoparticles or nanomaterial, they have size usually in the spectrum range of 1nm to 100nm. Researchers have developed different methods to synthesize nanoparticles, which includes bottom-up synthesis and top-bottom synthesis. Some of the well-known methods of nanoparticle synthesis are sol-gel, hydrothermal, chemical etching, mechanical milling, mechanochemical, laser ablation method, etc. shown in Figure1.2.

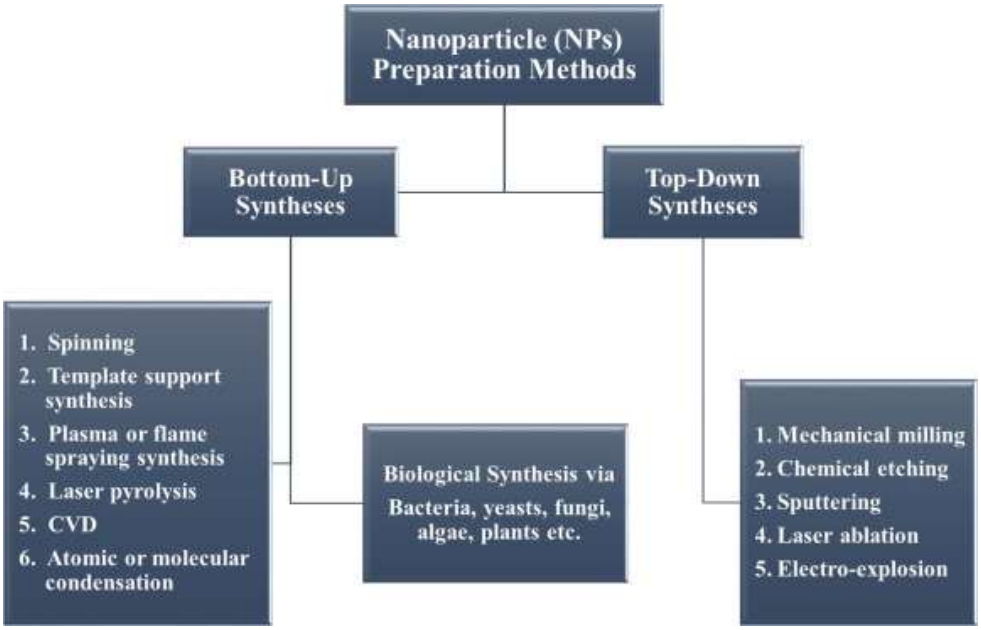

Figure 1.2 Methods for the preparation of nanoparticles [15]

1.3 Nanofluid

Nanofluid is a colloidal suspension of fluid and nanoparticles/nanomaterial suspended in it. Researchers have studied nanofluids containing various kinds of particles and fluids some of which are in the Figure 1.3. The fabrication of the nanofluid can be performed in two methods. In one method the nanofluid is prepared during the synthesis of nanoparticles by suspending nanoparticles in conventional fluid during generation process whereas in two steps method the nanometer-sized particles and nanofluid preparation take place independently. This technique prepares dry nanoparticles first and then they are added to fluid for nanofluid preparation.

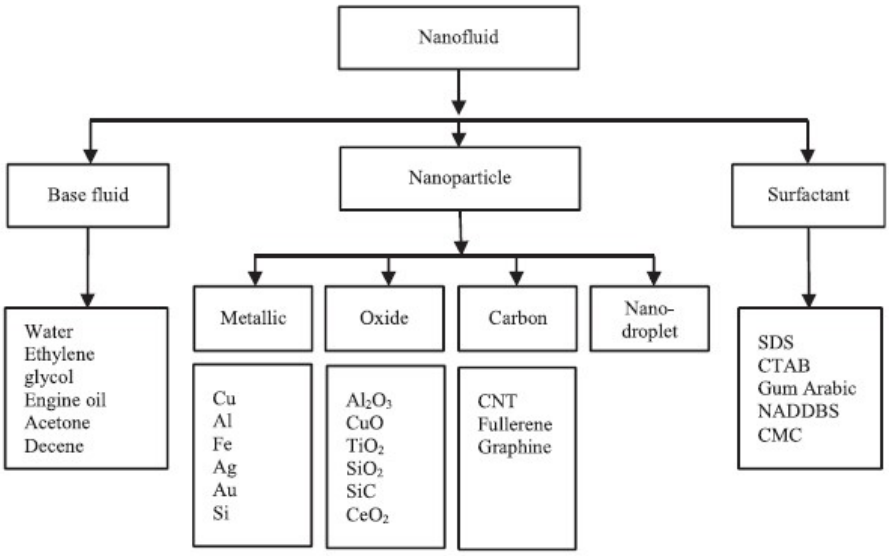

Figure 1.3 nanoparticles and nanofluids in literature [16]

1.4 Advantages of titanium dioxide nanofluid

Titanium dioxide nanofluid has grabbed the attention of researchers due to its outstanding physical and chemical properties. It has applications in different fields such as air purification, cosmetics, and printing, etc. It has no bad effects on human beings due to which it is known as safe material universally. Titanium dioxide has excellent chemical stability, resistance to acids, alkali and many organic erosions. Titanium dioxide has good dispensability in polar and non-polar fluid especially while using it along with surfactant [17]. Since dispersion in the fluid is one of the most important requirements of fluid to be used in industrial applications that's why many researchers have selected titanium dioxide nanofluid as a research subject, therefore titanium dioxide-based nanofluid can be considered as safe heat transport media. However, we need to know the thermal properties of the fluid for practical thermal applications.

1.5 Scope of study

In the recent past, researchers have worked hard to enhance conventional fluids thermo-physical properties which are used in industries for heat transfer purposes. One potential example is the heating load in the electronic appliances or engine cooling system which is increasing at a rapid pace while their size is constantly decreasing. Ethylene glycol, water, and engine oil, etc. are fluids mostly used in the industrial operations for heating

or cooling purposes. The main concern of conventional fluid is their low thermal conductivity. Nanofluid has improved properties (i.e. higher thermal conductivity) than conventional fluids, therefore it has shown better promise to be used in the industrial processes for improving heat transfer in the system. Nanofluids can be used in the electronics industry, automobile industries, solar collectors, fuel cells, nuclear reactors, and refrigeration systems.

1.6 Research Statement

To prepare nanofluid and thoroughly evaluate its stability and thermo-physical comprehensive literature review is performed. TiO_2 nanoparticles are prepared by the chemical technique. XRD and SEM results confirm the formation of spherical nanoparticles. The fabrication of the nanofluid is performed by adding the prepared nanoparticles to water along with CTAB surfactant and sonication for 1hr. The UV-Vis spectrometry results show nanofluid is stable for almost two weeks. Thermal properties of nanofluid are evaluated with the variation of particle concentration, shear rate, and temperature.

1.7 Objectives

The main objectives to carry out this research work are given below:

- Synthesis of TiO_2 nanoparticles.
- Characterization of TiO_2 nanoparticles by XRD, SEM, and EDS.
- Fabrication of TiO_2-H_2O nanofluid along with surfactant using ultra-sonication.
- The stability testing of TiO_2-H_2O nanofluid using UV-Vis spectroscopy.
- Determination of viscosity for TiO_2-H_2O nanofluid.
- Determination of Thermal Conductivity for TiO_2-H_2O nanofluid.

1.8 Organization of Thesis

Following pathway is adopted for studying the PCMs based TES system

- Chapter1 Introduction

Development of Nanofluid, Nanoparticles, Nanofluid, Advantages of titanium dioxide-based nanofluid, Scope of study, Research Statement, Objectives.

- Chapter 2 Literature Review

Preparation of the nanoparticles, Parameters affecting the shape, size, and phase of the particles, Nanofluid fabrication, Parameters affecting nanofluids stability, Stability measurement techniques for nanofluids, Viscosity, Parameters affecting the viscosity of the nanofluid, Thermal conductivity, Parameters affecting thermal conductivity.

- Chapter 3 Methodology

The methods followed to complete this research is explained in a flow chart.

- Chapter 4 Experimentation

Preparation of nanoparticles, Characterization, Surfactants, Preparation of nanofluid, Ultrasound probe sonicator, Stability, Thermo-physical properties of the nanofluid.

- Chapter 5 Results and Discussion

Characterization of nanoparticles, Stability evaluation of the nanofluid, Viscosity of nanofluid.

- Chapter 6 Conclusion and Recommendations

Summary

This section discusses the advancement in technologies like electronics, automobiles, refrigeration and the need for the development of new fluid like nanofluid for enhancement of heating or cooling. It further discusses the development of nanofluid, the advantages of using TiO_2 based nanofluid and potential applications of nanofluids.

References

[1] W. Yu and H. Xie, "A review on nanofluids: Preparation, stability mechanisms, and applications," *J. Nanomater.*, vol. 2012, 2012.

[2] H. M. Ali, M. U. Sajid, and A. Arshad, "Heat Transfer Applications of TiO_2 Nanofluids," *Appl. Titan. Dioxide*, 2017.

[3] S. A. Ahmed, M. Ozkaymak, A. Sözen, T. Menlik, and A. Fahed, "Improving car radiator performance by using TiO_2-water nanofluid," *Eng. Sci. Technol. an Int. J.*, vol. 21, no. 5, pp. 996–1005, 2018.

[4] H. M. Ali, M. D. Azhar, M. Saleem, Q. S. Saeed, and A. Saieed, "Heat transfer enhancement of car radiator using aqua based magnesium oxide nanofluids," *Therm. Sci.*, vol. 19, no. 6, pp. 2039–2048, 2015.

[5] N. A. Che Sidik, M. N. A. Witri Mohd Yazid, and R. Mamat, "Recent advancement of nanofluids in engine cooling system," *Renew. Sustain. Energy Rev.*, vol. 75, no. October 2016, pp. 137–144, 2017.

[6] K. Y. Leong, R. Saidur, S. N. Kazi, and A. H. Mamun, "Performance investigation of an automotive car radiator operated with nano fl uid-based coolants (nano fluid as a coolant in a radiator)," *Appl. Therm. Eng.*, vol. 30, no. 17–18, pp. 2685–2692, 2010.

[7] A. Ijam and R. Saidur, "Nano fluid as a coolant for electronic devices (cooling of electronic devices)," *Appl. Therm. Eng.*, vol. 32, pp. 76–82, 2012.

[8] A. M. Siddiqui, W. Arshad, H. M. Ali, M. Ali, and M. A. Nasir, "Evaluation of nanofluids performance for simulated microprocessor," *Therm. Sci.*, vol. 21, no. 5, pp. 2227–2236, 2017.

[9] T. Youse, F. Veysi, E. Shojaeizadeh, and S. Zinadini, "An experimental investigation on the effect of Al_2O_3- H_2O nano fluid on the efficiency of flat-plate solar collectors," vol. 39, pp. 293–298, 2012.

[10] A. Kasaeian, A. T. Eshghi, and M. Sameti, "A review on the applications of nano fluids in solar energy systems," *Renew. Sustain. Energy Rev.*, vol. 43, pp. 584–598, 2015.

[11] R. Saidur, T. C. Meng, Z. Said, M. Hasanuzzaman, and A. Kamyar, "International Journal of Heat and Mass Transfer Evaluation of the effect of nanofluid-based absorbers on direct solar collector," *Int. J. Heat Mass Transf.*,

vol. 55, no. 21–22, pp. 5899–5907, 2012.

[12] S. U. S. Choi and J. A. Eastman, “ENHANCING THERMAL CONDUCTIVITY OF FLUIDS WITH NANOPARTICLES *,” 1995.

[13] H. M. Nieh, T. P. Teng, and C. C. Yu, “Enhanced heat dissipation of a radiator using oxide nano-coolant,” *Int. J. Therm. Sci.*, vol. 77, pp. 252–261, 2014.

[14] R. Saidur, K. Y. Leong, and H. A. Mohammad, “A review on applications and challenges of nanofluids,” *Renew. Sustain. Energy Rev.*, vol. 15, no. 3, pp. 1646–1668, 2011.

[15] S. Mahata, S. S. Mahato, M. M. Nandi, and B. Mondal, “Synthesis of TiO_2 nanoparticles by hydrolysis and peptization of titanium isopropoxide solution,” *AIP Conf. Proc.*, vol. 1461, no. 1, pp. 225–228, 2011.

[16] D. Dey, P. Kumar, and S. Samantaray, “A review of nanofluid preparation, stability, and thermo-physical properties,” *Heat Transf. - Asian Res.*, vol. 46, no. 8, pp. 1413–1442, 2017.

[17] L. Yang and Y. Hu, “Toward TiO2 Nanofluids—Part 1: Preparation and Properties,” *Nanoscale Res. Lett.*, vol. 12, pp. 1–21, 2017.

Chapter 2

Literature Review

In past researchers have studied synthesis and characterization of the nanoparticles. Studies are also performed on stability, preparation, heat transport enhancement and thermal properties evaluation of the nanofluid. In this chapter, all techniques and methods for synthesis and characterization of nanofluid available in the literature are discussed.

2.1 Preparation of the nanoparticles

Researchers have developed different methods to synthesize nanoparticles namely sol-gel, hydrothermal, solvothermal, mechanical milling, mechanochemical, laser ablation method, etc. Mahshid et al. prepared titanium dioxide nanoparticles using a chemical method by the hydrolysis of titanium isopropoxide. The preparation was performed by titanium tetra isopropoxide added isopropanol to form an aqueous solution. Distilled water with various pH values was provided as a catalyst. HNO_3 or NH_4OH are used for pH values variation, the peptization temperatures was also varied to determine the effect of various pH and peptization temperature on particle size and phase of the particles. It was observed that the smaller size particles are formed in acidic solution and at lower temperatures while the size of the particles increases as the pH and peptization temperatures are increased. Anatase phase is formed at low temperature but the transformation to the rutile phase takes place at a temperature close to 600^oC and grows up to 800^oC [1]. Suresh et al. prepared TiO_2 nanoparticles using titanium tetra isopropoxide, ethanol, and hydrogen peroxide. It was found out that the spherical anatase phase nanoparticles are formed. The nanoparticles were characterized for phase and crystal size by XRD, morphology by SEM and particle size using TEM [2].

2.2 Parameters affecting the shape, size, and phase of the particles

There are different factors during the preparation of the nanoparticles which affect its size, shape, and phase. These factors include pH value, peptization or calcination temperature.

2.2.1 pH value

The acidic or basic solution used during the preparation of nanoparticles using chemical technique affects both the shape and size of the particles. It was found that smaller size particles are formed in acidic solution. The size of the nanoparticles increases as the pH value of the solution is raised [1].

2.2.2 Calcination temperature

The calcination temperature used during the synthesis of the nanoparticles affects the shape, size, and phase of nanometer size titanium dioxide particles. It is studied in the literature that particle size is directly related to the calcination temperature. Anatase phase titanium dioxide is formed below 600^{o}C. The transformation to the rutile phase takes place at a temperature close to 600^{o}C and grows up to 800^{o}C [1].

2.3 Nanofluid fabrication

Fabricated of nanofluid is performed using nanoparticles and fluid. It can be fabricated using two methods which are explained below.

2.3.1 One/single Step Method

Nanofluid preparation takes place during the synthesis of nanometer-size particles by suspending it in conventional fluid during the generation process. The single-step technique can be further separated into two methods namely physical and chemical method. The physical techniques include laser ablation, submerged arc, and vapors deposition. The chemical methods include chemical reactions to take place. This method is used for dry particle preparation but these can be upgraded to a one-step method by using base fluid containers instead of dry particle collectors [3]. It is expected that a single step technique will possess improved stability as it does not use drying and dispersion, however, it has side effects that are more dangerous to be used in certain environments that restrict its application.

2.3.2 Two-step method

Most of the researchers applied a two-step technique for nanofluid fabrication [4]–[12]. In this method, the nanometer-sized particles and nanofluid preparation take place independently. This technique prepares dry nanoparticles first and then they are added to fluid for nanofluid preparation but dispersion issues can take place which will affect

the stability of the nanofluid, therefore some dispersion methods such as an ultrasonic probe or ultrasonic bath are used for dispersion of the solution. This method is mostly applied because of substantial improvement in dispersion techniques and its adaptability. The literature suggests better properties and performance of the nanofluid prepared in two steps as compared to those prepared in single steps [3].

2.4 **Parameters affecting nanofluids stability**

The most important thing for the fabrication of nanofluid is its stability for its practical application. Some of the factors affecting the nanofluid stability are explained as under.

2.4.1 Ultrasonic vibration

Nanofluid is prepared using nanoparticles and fluid. The problem faced is particle agglomeration and it's settling down to the bottom. The ultrasonic vibration disperses nanoparticles in a nanofluid. It is of two types i.e. ultrasonic bath and ultrasonic probe vibration. It is found that the nanofluid has better stability after ultrasonic vibration [3]. The probe type of sonication can be performed with pulses and without pulses. It is found out that the vibration performed continuously or without pulses shows better stability as compared to the ultrasonic vibration performed with pulses [13]. Mechanical stirring can also be used for dispersion of nanofluid and the results showed that the dispersion performed by ultrasonic vibration at 25 kHz for 48 hours is more stable than the dispersion performed using mechanical stirring in Al_2O_3-H_2O and TiO_2-H_2O [14].

2.4.2 Surfactants

The stability of the nanofluid is improved by using Surfactant or dispersant**.** The nanoparticles surfaces of the can be modified by adding dispersant or surfactant to it, which reduces agglomeration of particles by electrostatic repulsion or static hindrance performed by the surfactant molecules and hence can result in the formation of the stable nanofluid [3]. The most frequently used surfactants are SDS, Acetic acid (AA), CTAB, polyvinylpyrrolidone (PVP), SDBS and oleic acid. Azadeh et al. prepared nanofluid by TiO_2 nanoparticles, distilled water, SDS surfactants, ultrasonic bath, and ultrasonic horn. The results showed that the surfactants along with the ultrasonic bath and horn increase the stability of nanofluid. The best results were observed for surfactants addition in the same amount as nanoparticles along with an ultrasonic bath.

Das et al. fabricated nanofluid with CTAB, acetic acid (AA) and SDS as surfactants [8]. They examined that the most stable nanofluid was obtained using CTAB and acetic acid as a surfactant. The nanofluid prepared using rutile rod-shaped and anatase spherical shaped TiO_2 nanoparticles added to water can be kept stable for 286hrs using SDS surfactant. It is also observed that if mass ratio of titanium dioxide and SDBS is kept 0.3 best dispersion is obtained when CTAB, SDBS & PVP surfactants were added to distilled water and dispersion was tested [15]. TiO_2 nanoparticles stability in organic fluids is observed to be better in the two-step method than one step method when propionic acid and n-hexylamine are used as the surfactant which modifies the surface of nanoparticles [16].

2.4.3 pH value

The variation of the base fluid to be acidic or basic also affects particle dispersion in the fluid and can affect the stability of nanofluid. The dispersion of the particles is performed by electrostatic repulsion obtained by adjusting the pH value. This method results in a higher zeta potential value [17]. He et al. showed that nanofluid stability can be highly increased by increasing the fluid pH value up to 11, which can result in the prevention of deposition and agglomeration and possible fouling of the tube. The optimal value of the pH can result in stable nanofluid for few months. Vakili et al. & sen et al. also checked nanofluid stability at 11 pH value and they observed that titanium dioxide-based nanofluid is very stable in this condition. The pH value adjustment will restrict the application of the nanofluid in many applications because of the corrosion and safety in alkaline and acidic conditions[18] [19].

2.4.4 Combination of processes

All of these processes can be performed on the nanofluid in order to get the most stable nanofluid [20]. In most cases, the pH adjustment is ignored as it can affect the application of nanofluid in a certain environment. Ultrasonic vibration and surfactants are used to combine during nanofluid preparation to obtain stable nanofluid.

2.5 **Stability measurement techniques for nanofluids**

In the past researchers have studied nanofluid stability using different methods. Stability is one of the basic concerns in the practical application of the nanofluid. The nanoparticle agglomeration not only settles down but may also cause clogging in the

heat exchanger. Study and analyses of stability are necessary for nanofluid before using it in practical applications. Some of the methods used for the evaluation of nanofluid stability are as under.

2.5.1 Spectral absorbency

It is one of the efficient techniques to analyze the nanofluid stability. Literature suggests a linear relationship between spectral absorbency and the concentration of nanometer-sized particles in the nanofluid. If the nanoparticles dispersed in nanofluid have their characteristic bandwidth in the range of 190nm to 1100nm then its stability can be reliably examined by applying UV-Vis spectroscopy. The supernatant particle concentration in nanofluid variation with sediment time can be received from measuring its absorbance. A linear relation is found between the absorbance and the particle nanofluid concentration. The benefit of this method is its ability to give a quantitative concentration of the nanofluid [21]. Huang et al. showed that the stability of copper, alumina suspension can be determined with absorbency spectroscopy using UV Vis spectrophotometer on sample suspended for 24hours.Hwang et al. performed the stability study using UV Vis spectrophotometry. The results confirmed that nanofluid stability was strongly a function of particle properties & fluid and the use of surfactant along them can improve the nanofluid stability performance [22].

2.5.2 Zeta potential analysis

The zeta potential is significant because the value obtained from zeta potential can relate to the stability of the dispersed colloid. In this method, the nanofluid with higher zeta potential value will be stabilized electrically while those having lower value will flocculate or coagulate. Some of the researchers have suggested the value of 25mV (Positive or negative) as an arbitrary value that separates highly charged surfaces from low charged surfaces. The zeta value in the range of 40mV to 60mV is considered as stable, while colloids having the zeta potential value above 60mV have excellent stability [21]. Kim et al. prepared Au water nanofluid which has high stability due to its large negative zeta potential value [23]. The table represents the stability value range for zeta potential [24].

Zeta potential value (mV)	colloid Stability behavior
0 to ±5	rapidly flocculating or coagulating
±10 to ±30	incipiently Instable
±30 to ±40	moderately stable
±40 to ±60	stable
More than ±61	excellently stable

2.5.3 Sedimentation photo capturing method

The easiest technique for the nanofluid stability evaluation is by using the sedimentation method [25][26]. The particles sedimentation volume/weight in a fluid under an external force represents the stability of the nanofluid. Stable nanofluid is fabricated if particle concentration in it remains constant [21]. The photograph of the sedimentation taken by using a camera in a beaker is another method for the evaluation of the stability of the nanofluid [27].

2.6 **Viscosity**

This is one of the most important properties needs to be known for the practical application of the nanofluid in industrial processes. It determines the power requirement of the pump and the fluid pressure drop. It is the resistance of one fluid layer to another. Literature suggests that the nanofluid viscosity will be higher compared to a conventional fluid. The increase in viscosity will result in a higher power requirement of the pump and it can decrease the rate of heat transfer in some cases. There are different parameters that affect the viscosity of the nanofluid which are explained below.

2.7 **Parameters affecting the viscosity of the nanofluid**

Some of the factors affecting the viscosity of the nanofluid investigated by different researchers so far are particle loading, shear rate, temperature, morphology, surfactants, and dispersion technique.

2.7.1 Particle loading

The particle loading or concentration affects the viscosity of the nanofluid which is studied experimentally by different researchers. According to most of the scientists, the viscosity varies directly with the particle loadings in a nanofluid. The viscosity of the nanofluid is found to be increasing with nanoparticles concentration in the nanofluid. Some of the researchers observed linear increment in viscosity while the others found parabolic increment with the amount of particle loading. Jarahnejad et al. performed an experiment to check the variation of viscosity with the nanofluid particle loading of 3wt%, 6wt% and 9 wt% at 20^{o}C. They determined that fluid becomes more viscous with the amount of particle loading [28]. Das et al. results were the same they said that viscosity has a direct relation with the concentration of the particles used. They observed the viscosity dependence upon conventional fluid [7].

2.7.2 Temperature of nanofluid

The viscosity variation with temperature of nanofluid is also investigated by many researchers. Pritam Das et al examined the variation of nanofluid viscosity prepared with particles having a size of 10nm to 40nm by a two-step method. The results confirmed an inverse relation of viscosity and temperature of the sample. Jarahnejad et al. experimentation for checking viscosity variation with the temperature of the nanofluid at different particle loading of 3wt%, 6wt%, and 9 wt% found that with particle loading the viscosity increases but relative viscosity almost remained constant with temperature [28]. The effect that viscosity is independent of temperature is experienced by many researchers. Teng et al. found that by raising the temperature from 10^{o}C to 40^{o}C for TiO_2 nanofluid at 0.5 wt% the increase of 8.2% to 16% was observed in relative viscosity [29]. Cieśliński et al. showed that oil-based nanofluid viscosity was independent of temperature when varied from 20^{o}C to 40^{o}C [30]. Yapici et al. determined that the variation in viscosity with temperature is also dependent upon the shear rate. They found independency in viscosity with the temperature at a higher shear rate while at low shear rate viscosity was dependent upon the temperature of the nanofluid sample [24].

2.7.3 Particle size and shape

The viscosity variation with the particle shape and size for nanofluid is not widely studied. Chen et al. investigated the variation for spherical with size 25nm and rod-shaped (10 × 100) titanium dioxide nanofluid with both ethylene glycol and water fluids. The results showed the increase in viscosity for spherical TiO_2 from 0.5 to 23% when concentrations were kept in the range of 0.1vol% to 1.86vol% while for rod-like TiO_2 the increase in viscosity was observed to be from 1 to 82% for the concentration of 0.vol% to 0.6vol% [32].

2.7.4 Shear rate

Most of the researchers investigated that if the nanofluid is Newtonian or non-Newtonian at higher shear rates. Yapici et al. examined the viscosity of TiO_2 –water at 9wt% and Ti O_2 –PEG200 nanofluid with different surfactants against time. They found that the TiO_2 –PEG200 nanofluid remained Newtonian at higher shear rates and low temperature while it became non-Newtonian at a low shear rate and higher temperatures [31]. Said et al. investigated TiO_2 nanofluid at a concentration of 0.1vol%. They found that the nanofluid were Newtonian at 55^oC while below this temperature it was non-Newtonian for 0.3vol% [33]. Das et al. prepared TiO_2 nanofluid with different surfactants and investigated its viscosity variation with shear rate. They found that nanofluid viscosity increases with the rise of shear rate constant temperature of 24^oC when varied from 76 s^{-1} to 760 s^{-1} [7].

2.7.5 Surfactants

According to most of the researchers the nanofluid viscosity changes with the surfactant. Jarahnejad et al. examined the effect of surfactant namely polycarboxylate and trioxidecane on TiO_2 nanofluid viscosity. They observed that the TiO_2- water nanofluid viscosity of 9wt% was slightly raised by the use of surfactant and in the temperature range of 20^oC to 50^oC viscosity can be greatly increased by the use of these surfactants [28]. Ghadimi et al. investigated 0.1vol% TiO_2 nanofluid viscosity variation with surfactant. They found that the viscosity of the nanofluid is raised using the SDS surfactant [20] . Ling et al. in their experimentation showed that TiO_2 nanofluid viscosity with lower concentration will be slightly decreased by the addition of SDBS or OP-10 surfactant.

2.7.6 Base fluid

The base fluid variation also affects the viscosity of the nanofluid which is investigated by many researchers. Chen et al. evaluated through experiment the effect of base fluid on viscosity. The results showed that TiO_2 viscosity was lower in ethylene glycol nanofluid compared to water-based nanofluid. It was observed that the increase in viscosity for the higher viscosity base fluid is smaller than the lower viscosity base fluid [32].

2.8 Thermal conductivity

It shows the heat conduction capability of the material. The thermal conductivity of metals is better than fluids. The thermal conductivity of copper is 700 times more than that of water and 3000 times more than engine oil as shown in Figure 2.1 thus it can be said that fluids suspension containing metal and fluid will definitely possess more thermal conductivity compared to fluid alone [34]. In past, people tried to add millimeter size or micrometer size metals to the fluid to improve its heat transfer properties but the problems faced were aggregation, sedimentation, poor dispensability and adhering to the walls of the system which can result in lowering fluid's thermal conductivity. The thermal conductivity measured by different methods shows different results because of sedimentation, aggregation, particle diameter and nanofluid preparation . Nor Azwadi Che Sidik et al. reviews many papers related to nanofluid used in the engine system. It was found that nanofluid improve engine oil's or water's thermal conductivity up to 50% as compared to a normal fluid. The nanofluid's thermal conductivity varies with nanoparticles concentration in nanofluid, nanofluids sample temperature, nanoparticles size, and shape in the nanofluid [35].

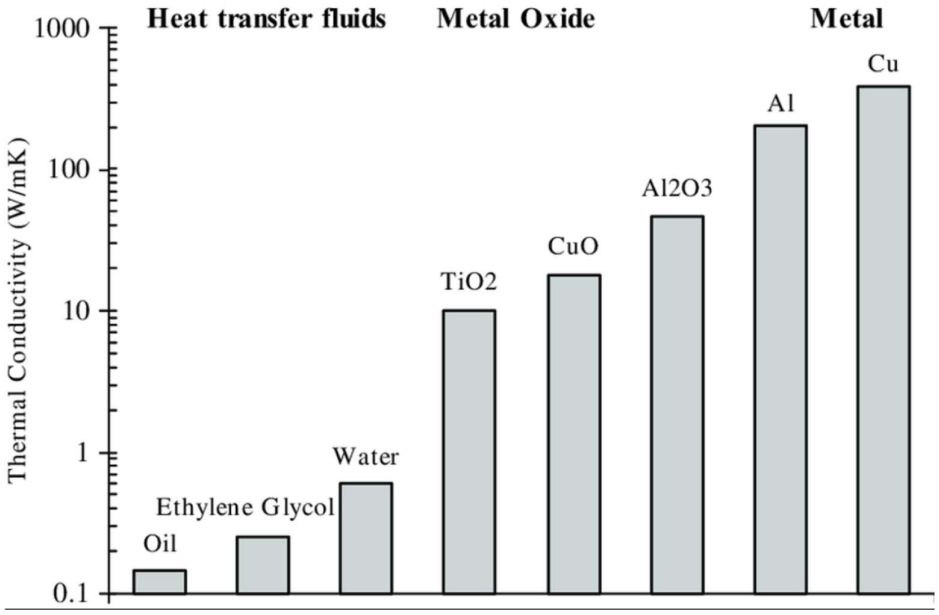

Figure 2.1 Thermal conductivity of different materials [3]

2.9 **Parameters affecting thermal conductivity**

Nanofluid thermal conductivity is affected by many factors. Few of the parameters affecting nanofluids thermal conductivity are explained as under.

2.9.1 Particle concentration

The nanofluids thermal conductivity variation with the particle loadings is investigated by different researchers. Mostly it is observed that nanofluids' thermal conductivity becomes lower as the particle concentrations are lowered. Pritam Das et al. nanofluid prepared along with different surfactants shows that solid volume fraction has a direct relation with the nanofluids thermal conductivity [7]. Chopkar et al performed an experiment on nanofluid based on ethylene glycol and confirmed that thermal conductivity was almost doubled by the addition of nanoparticles [36]. Duangthongsuk and Wongwises examined that the TiO_2 water nanofluid thermal conductivity becomes more with raising particle concentration [37]. Sridhara et al. reviewed different papers related to nanofluid s thermal conductivity. The outcomes of the study were that the thermal conductivity increases up to 5% volume concentration of alumina nanoparticles and in some cases, it increases up to 10% while in other it decreases for 6 to 10% volume concentration. Eastman et al. evaluated thermal conductivity of oil and water with various kinds of nanoparticles. Thermal conductivity was enhanced upto 60% with

5vol% particle loading [38]. According to Lee et al. there is a linear rise in thermal conductivity below 0.05vol% particle loading and about 20% thermal conductivity enhancement in nanofluid containing ethylene glycol at 4vol% concentration of CuO nanoparticles [38]. Karthikeyan et al found 31% to 54% enhancement in ethylene glycol's and water's thermal conductivity using 1vol% of CuO nanoparticles [40]. Utomo et al observed no enhancement in TiO_2 water and Al_2O_3 water nanofluids' thermal conductivity because of particle aggregation [41]. Fedele et al experimental results shows that TiO_2 water nanofluid thermal conductivity is directly related to concentration of nanoparticles. Almost 38.1% enhancement was observed in thermal conductivity using 35wt% nanoparticles [42].

2.9.2 Temperature

The thermal conductivity variation with the temperature is also widely studied in the past. The literature suggests that temperature greatly affects the thermal conductivity of the nanofluid as both the particles and fluid thermal conductivity is dependent upon temperature. Das et al. examined experimentally the variation of thermal conductivity with the temperature of the nanofluid for Al_2O_3 and CuO nanoparticles. According to their results, the thermal conductivity enhancement is increased from 2% to 10.8% when the temperature was raised from 21°C to 51°C at concentration of 1vol%. They also observed that thermal conductivity enhancement at 4vol% was increased from 9.4% to 24.3% when the temperature of the sample was raised from 21°C to 51°C [7][8]. Li and Peterson also studied the effect of temperature on the thermal conductivity of Al_2O_3 and CuO and water-based nanofluid. The result showed almost three times increase in thermal conductivity when the mean temperature was raised from 27°C to 34.7°C and they observed that the thermal conductivity increased with the rise in temperature at a constant concentration [43]. Agarwal et al. performed Sensitivity analysis which showed that the thermal conductivity is sensitive to change in temperature and volume concentration. Water-based nanofluid is more sensitive as compared to engine oil and ethylene glycol nanofluid. Rashmi et al. found 100%-250% enhancement in thermal conductivity using CNT nanoparticles in the temperature range of 25°C to 60°C. It can be concluded that the thermal conductivity of the nanofluid increases when its temperature is raised [44].

2.9.3 Base fluid

The base fluid thermal conductivity also affects the thermal conductivity of the nanofluid. It has been found in the literature that the increase in nanofluid thermal conductivity is not high in fluids having a larger value of thermal conductivity. Wang et al. performed experimentation to determine the rise in thermal conductivity using different fluids such as engine oil, water, ethylene glycol, and vacuum pump oil along with Al_2O_3 and CuO nanoparticles. The high-value thermal conductivity was found in the order of ethylene glycol, water, engine oil, and vacuum pump oil respectively [45]. Xie et al. performed an experiment for thermal conductivity evaluation of distilled ethylene glycol, water, and decene based nanofluids. The thermal conductivity of the water was lowest followed by ethylene glycol and decene. This behavior is due to the fact that water has the highest thermal conductivity followed by ethylene glycol and decene [46]. Thus, conclusion from the above can be that the rise in thermal conductivity decreases as the base fluid having a higher value of thermal conductivity is used. Agarwal et al. Found about a 40% rise in thermal conductivity for nanofluid containing water measured by KD 2 pro while for nanofluid containing ethylene glycol the rise in thermal conductivity was 27% and 19% increase was observed in engine oil based nanofluid.

2.9.4 Particle size

The thermal conductivity is affected by the particle size variation in the nanofluid. The expectation is that as the size of the nanoparticles is lowered the thermal conductivity will be raised because of increased area. Wang et al. dispersed Al_2O_3 (28nm) and CuO (23nm) in different fluids. They observed that the thermal conductivity of CuO is greater than Al_2O_3 due to the small size of the particles. However, there are some contradicting results found by some researchers [45]. Chopkar et al. found the inverse relation between thermal conductivity and particle size of the nanoparticles [36]. Xie et al. evaluated the enhancement in thermal conductivity using cylindrical, spherical shape SiC particles having 600nm and 20nm size respectively. The results confirmed thermal conductivity enhancement of 22.9% at 4vol% for 600nm cylindrical particles and about 15.8% enhancement at 4.2vol% for 20nm spherical SiC nanoparticles. This thermal conductivity behavioral contradiction can be explained in such a way that the smaller

particles joined together and form a cluster severely. Clustering may cause thermal conductivity to increase but the high amount of clusters will have the opposite effect and may result in sedimentation of the nanoparticles [46].

2.9.5 Particle shape

Thermal conductivity variation with the shape of nanoparticles is also studied by many researchers. Although the mostly cylindrical or spherical shapes of the nanoparticles are used. Xie et al. determined enhancement in thermal conductivity by the application of cylindrical and spherical shaped SiC nanoparticles having a size of 600nm, 20nm respectively. They observed 22.9% thermal conductivity enhancement at 4vol% for 600nm cylindrical particles and about 15.8% enhancement for 4.2vol% was observed for 20nm spherical SiC nanoparticles [47]. Murshed et al. evaluated thermal conductivity variation with the shape of TiO_2 nanoparticles. The mostly cylindrical or spherical shape of the nanoparticles was used. Almost 29.7% enhancement occurred in thermal conductivity for spherical shaped particles while 32.8% enhancement was recorded in cylindrical shape TiO_2 particles at 5vol% concentration. These results show that cylindrical-shaped nanoparticle has better performance than spherical shaped particles because of higher surface area [48].

Summary

This section presents a comprehensive literature study about the synthesis of nanoparticles, fabrication, and stability of the nanofluid. It further discusses the factors which affect the size and shape of nanoparticles during synthesis. It also discusses different parameters that affect the fabrication, thermal properties, and stability of the nanofluid.

References

[1] S. Mahata, S. S. Mahato, M. M. Nandi, and B. Mondal, "Synthesis of TiO_2 nanoparticles by hydrolysis and peptization of titanium isopropoxide solution," *AIP Conf. Proc.*, vol. 1461, no. 1, pp. 225–228, 2011.

[2] S. Sagadevan, "Synthesis and Electrical Properties of TiO2 Nanoparticles Using a Wet Chemical Technique," *Am. J. Nanosci. Nanotechnol.*, vol. 1, no. 1, p. 27, 2013.

[3] L. Yang and Y. Hu, "Toward TiO_2 Nanofluids—Part 1: Preparation and Properties," *Nanoscale Res. Lett.*, vol. 12, pp. 1–21, 2017.

[4] K. Y. Leong, R. Saidur, S. N. Kazi, and A. H. Mamun, "Performance investigation of an automotive car radiator operated with nano fl uid-based coolants (nano fl uid as a coolant in a radiator)," *Appl. Therm. Eng.*, vol. 30, no. 17–18, pp. 2685–2692, 2010.

[5] M. Arulprakasajothi, K. Elangovan, K. H. Reddy, and S. Suresh, "Heat transfer study of water-based Nanofluids containing titanium oxide nanoparticles," *Mater. Today Proc.*, vol. 2, no. 4–5, pp. 3648–3655, 2015.

[6] N. Kaewgabkam, N. Jaitanong, and S. Narksitipan, "Preparation and Characterization of Cement-TiO_2 Composites," vol. 804, pp. 133–136, 2015.

[7] P. K. Das, A. K. Mallik, R. Ganguly, and A. K. Santra, "Stability and thermophysical measurements of TiO_2 (anatase) nanofluids with different surfactants," *J. Mol. Liq.*, vol. 254, pp. 98–107, 2018.

[8] P. K. Das, A. K. Mallik, R. Ganguly, and A. K. Santra, "Synthesis and characterization of TiO_2-water nanofluids with different surfactants," *Int. Commun. Heat Mass Transf.*, vol. 75, pp. 341–348, 2016.

[9] S. A. Ahmed, M. Ozkaymak, A. Sözen, T. Menlik, and A. Fahed, "Improving car radiator performance by using TiO_2-water nanofluid," *Eng. Sci. Technol. an Int. J.*, vol. 21, no. 5, pp. 996–1005, 2018.

[10] H. M. Nieh, T. P. Teng, and C. C. Yu, "Enhanced heat dissipation of a radiator using oxide nano-coolant," *Int. J. Therm. Sci.*, vol. 77, pp. 252–261, 2014.

[11] H. Setia, R. Gupta, and R. K. Wanchoo, "Thermophysical properties of TiO_2-water based nanofluids," *AIP Conf. Proc.*, vol. 1393, pp. 267–268, 2011.

[12] G. M. Moldoveanu, A. A. Minea, M. Iacob, C. Ibanescu, and M. Danu,

"Experimental study on viscosity of stabilized Al2O3, TiO_2 nanofluids and their hybrid," *Thermochim. Acta*, vol. 659, pp. 203–212, 2018.

[13] B. Tajik, A. Abbassi, M. Saffar-avval, and M. A. Najafabadi, "Ultrasonic properties of suspensions of TiO_2 and Al_2O_3 nanoparticles in water," *Powder Technol.*, vol. 217, pp. 171–176, 2012.

[14] G. A. Longo and C. Zilio, "Experimental measurement of thermophysical properties of oxide – water nano-fluids down to ice-point," *Exp. Therm. Fluid Sci.*, vol. 35, no. 7, pp. 1313–1324, 2011.

[15] S. Mo, Y. Chen, L. Jia, and X. Luo, "Investigation on crystallization of TiO_2 – water nanofluids and deionized water," *Appl. Energy*, vol. 93, no. 100, pp. 65–70, 2012.

[16] N. Nakayama and T. Hayashi, "Preparation of TiO_2 nanoparticles surface-modified by both carboxylic acid and amine : Dispersibility and stabilization in organic solvents," vol. 317, pp. 543–550, 2008.

[17] R. Choudhary, D. Khurana, A. Kumar, and S. Subudhi, "Stability analysis of Al_2O_3 / water nanofluids," vol. 8080, no. February, 2017.

[18] M. Vakili, A. Mohebbi, and H. Hashemipour, "Experimental study on convective heat transfer of TiO_2 nanofluids," *Heat Mass Transf. und Stoffuebertragung*, vol. 49, no. 8, pp. 1159–1165, 2013.

[19] S. Sen, V. Govindarajan, C. J. Pelliccione, J. Wang, E. V Timofeeva, and D. J. Miller, "Surface modification approach to TiO_2 nanofluids with high particle concentration , low viscosity and electrochemical activity," 2015.

[20] A. Ghadimi and I. H. Metselaar, "The influence of surfactant and ultrasonic processing on improvement of stability, thermal conductivity and viscosity of titania nanofluid," *Exp. Therm. Fluid Sci.*, vol. 51, pp. 1–9, 2013.

[21] W. Yu and H. Xie, "A review on nanofluids: Preparation, stability mechanisms, and applications," *J. Nanomater.*, vol. 2012, 2012.

[22] Y. Hwang *et al.*, "Stability and thermal conductivity characteristics of nanofluids," vol. 455, pp. 70–74, 2007.

[23] H. Jin, I. Cheol, and J. Onoe, "Characteristic stability of bare Au-water nanofluids fabricated by pulsed laser ablation in liquids," vol. 47, pp. 532–538, 2009.

[24] “PERFORMANCE STUDY OF CONICAL STRIP INSERTS IN TUBE HEAT EXCHANGER.”

[25] X. Wei and L. Wang, “Particuology Synthesis and thermal conductivity of microfluidic copper nanofluids,” *Particuology*, vol. 8, no. 3, pp. 262–271, 2010.

[26] X. Li, D. Zhu, and X. Wang, “Evaluation on dispersion behavior of the aqueous copper nano-suspensions,” vol. 310, pp. 456–463, 2007.

[27] Y. Li, S. Tung, E. Schneider, and S. Xi, “A review on development of nanofluid preparation and characterization,” vol. 196, pp. 89–101, 2009.

[28] M. Jarahnejad, E. B. Haghighi, and M. Saleemi, “Experimental investigation on viscosity of water-based Al_2O_3 and TiO_2 nanofluids,” no. 2001, 2015.

[29] T. P. Teng, Y. H. Hung, C. S. Jwo, C. C. Chen, and L. Y. Jeng, “Pressure drop of TiO_2 nanofluid in circular pipes,” *Particuology*, vol. 9, no. 5, pp. 486–491, 2011.

[30] K. Ronewicz, “Measurement of temperature-dependent viscosity and thermal conductivity of alumina and titania thermal oil nanofluids Introduction,” vol. 36, no. 4, pp. 35–47, 2015.

[31] K. Yapici, N. K. Cakmak, N. Ilhan, and Y. Uludag, “Rheological characterization of polyethylene glycol based TiO_2 nanofluids,” vol. 26, no. 4, pp. 355–363, 2014.

[32] H. Chen, S. Witharana, Y. Jin, C. Kim, and Y. Ding, “Predicting thermal conductivity of liquid suspensions of nanoparticles (nanofluids) based on rheology,” vol. 7, pp. 151–157, 2009.

[33] Z. Said *et al.*, “Performance enhancement of a Flat Plate Solar collector using TiO2 nanofluid and Polyethylene Glycol dispersant,” *J. Clean. Prod.*, 2015.

[34] T. Youse, F. Veysi, E. Shojaeizadeh, and S. Zinadini, “An experimental investigation on the effect of Al_2O_3- H_2O nano fluid on the efficiency of flat-plate solar collectors,” vol. 39, pp. 293–298, 2012.

[35] N. A. Che Sidik, M. N. A. Witri Mohd Yazid, and R. Mamat, “Recent advancement of nanofluids in engine cooling system,” *Renew. Sustain. Energy Rev.*, vol. 75, no. October 2016, pp. 137–144, 2017.

[36] M. Chopkar, S. Sudarshan, P. K. Das, and I. Manna, “Effect of Particle Size on

Thermal Conductivity of Nanofluid," vol. 39, no. July, 2008.

[37] W. Duangthongsuk and S. Wongwises, "International Journal of Heat and Mass Transfer An experimental study on the heat transfer performance and pressure drop of TiO_2 -water nanofluids flowing under a turbulent flow regime," *Int. J. Heat Mass Transf.*, vol. 53, no. 1–3, pp. 334–344, 2010.

[38] J. A. Eastman, U. S. Choi, S. Li, L. J. Thompson, and S. Lee, "No Title," vol. 457, pp. 3–11.

[39] S. Lee, "Measuring Thermal Conductivity of Fluids Containing Oxide Nanoparticles," vol. 121, no. May 1999, 2013.

[40] N. R. Karthikeyan, J. Philip, and B. Raj, "Effect of clustering on the thermal conductivity of nanofluids," vol. 109, pp. 50–55, 2008.

[41] A. Durairajan, T. Kavitha, A. Rajendran, and L. A. Kumaraswamidhas, "Heat transfer intensification by Nanofluids- an Outline," vol. 73, no. November, pp. 711–712, 2014.

[42] L. Fedele, L. Colla, and S. Bobbo, "Viscosity and thermal conductivity measurements of water-based nanofluids containing titanium oxide nanoparticles ´ thermique de Mesures de la viscosite nanofluides aqueuses contenant des nanoparticules d ' oxyde de titane," *Int. J. Refrig.*, vol. 35, no. 5, pp. 1359–1366, 2012.

[43] C. H. Li and G. P. Peterson, "Experimental investigation of temperature and volume fraction variations on the effective thermal conductivity of nanoparticle suspensions (nanofluids) Experimental investigation of temperature and volume fraction variations on the effective thermal conductivity of nanoparticle suspensions," vol. 084314, 2006.

[44] W. Rashmi, M. Khalid, S. S. Ong, and R. Saidur, "Preparation, thermo-physical properties and heat transfer enhancement of nanofluids," *Mater. Res. Express*, vol. 1, no. 3, 2014.

[45] X. Wang and X. Xu, "Thermal Conductivity of Nanoparticle – Fluid Mixture," vol. 13, no. 4, 1999.

[46] H. Xie *et al.*, "Nanofluids containing multiwalled carbon nanotubes and their enhanced thermal conductivities Nanofluids containing multiwalled carbon nanotubes and their enhanced thermal conductivities," vol. 4967, 2003.

[47] H. Xie, J. Wang, T. Xi, and Y. Liu, “Thermal Conductivity of Suspensions Containing Nanosized SiC Particles,” vol. 23, no. 2, 2002.

[48] S. M. S. Murshed, K. C. Leong, and C. Yang, “Enhanced thermal conductivity of TiO 2 — water based nanofluids,” vol. 44, pp. 367–373, 2005.

Chapter 3

Methodology

The flow chart in the figure shows the complete methodology of this research work to achieve our objectives. The framework followed in the current study begins with a thorough literature review of different types of nanoparticles, surfactants, and nanofluids. The methods used for the preparation of the titanium dioxide nanoparticles, fabrication of the nanofluid and stability evaluation of the nanofluid were studied in detail.

Titanium dioxide nanoparticles were prepared by the wet chemical method using titanium tetra isopropoxide, ethanol, and hydrogen peroxide. The nanoparticles' shape, crystallite size, and elemental composition were characterized using SEM, XRD, and EDS respectively.

Nanofluid is fabricated by the two-step technique by the sonication of water, titanium dioxide nanoparticles, and cetyl tri-methyl ammonium bromide surfactant. The nanofluid stability is evaluated using UV-Vis spectroscopy and sedimentation photo capturing.

The viscosity of the nanofluid is examined using a Brookfield type of viscometer. The viscosity of the nanofluid is evaluated in the temperature range of 30ºC, 40 ºC, 60 ºC, and 80 ºC at a constant shear rate of $100s^{-1}$. The viscosity of the nanofluid is also studied at the shear rate of 50 s^{-1}, 100 s^{-1}, 150 s^{-1}, 200 s^{-1} and 245 s^{-1} at a constant temperature of 30 ºC. The variation of viscosity is also determined for different concentrations of the nanofluid.

The thermal conductivity of the nanofluid is measured. The measured value of thermal conductivity of the nanofluid is compared with different models proposed in literature. The variation of thermal conductivity with particle loading is also studied.

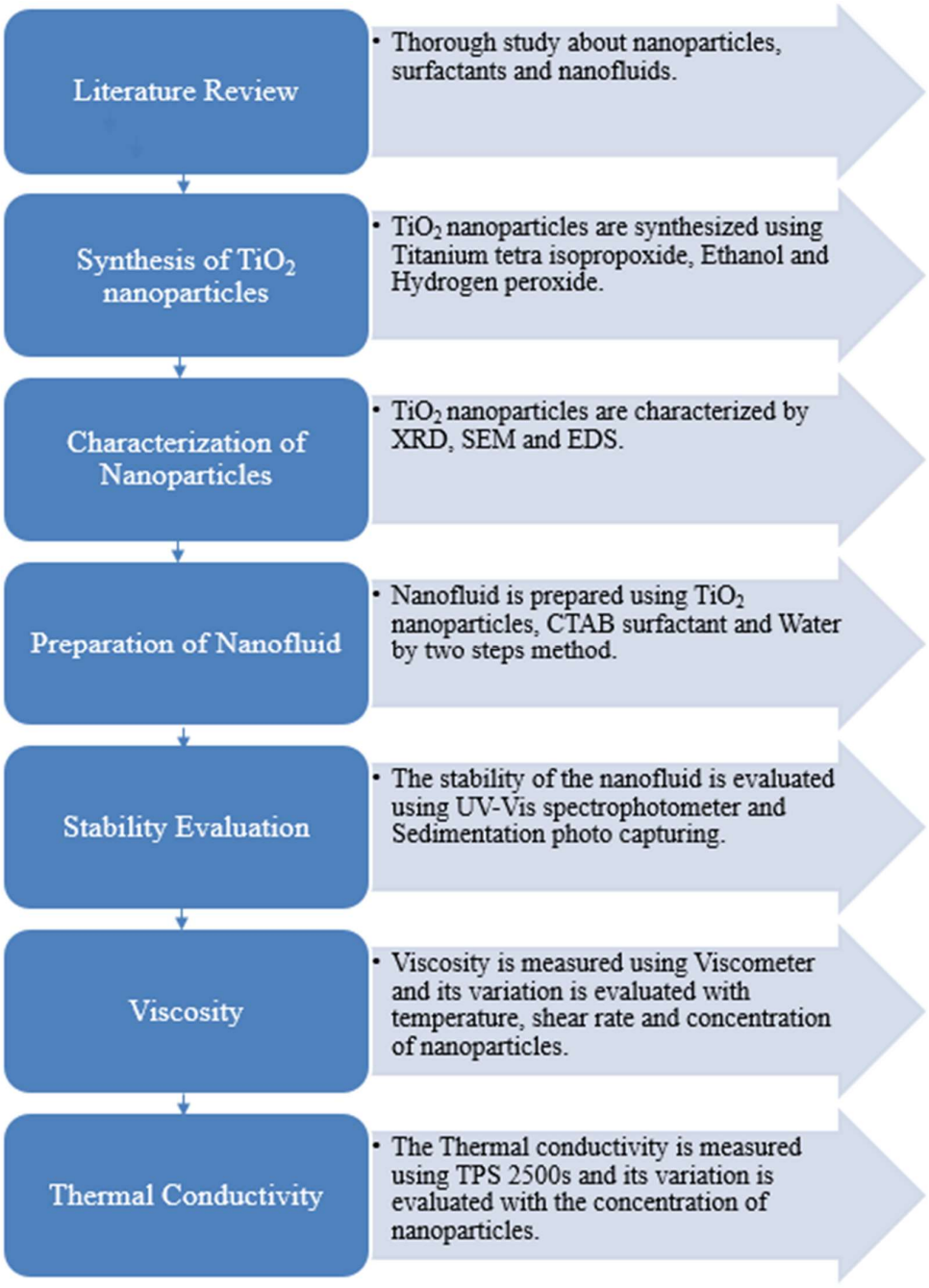

Figure 3.1 Flow diagram of research work

Summary

The methodology followed to achieve our objectives are discussed in this section. The nanoparticle preparation, characterization, nanofluid fabrication, its stability characteristics, and its thermal properties namely thermal conductivity and viscosity are discussed.

Chapter 4

Preparation and Characterization

4.1 Preparation of nanoparticles

TiO_2 nanoparticles were prepared by using a chemical method. The chemical used in the synthesis of TiO_2 nanoparticles were Titanium tetra isopropoxide TTIP (97% purity supplied by sigma Aldrich), Ethanol (99% supplied by Merck) and hydrogen peroxide (35% supplied by BDH laboratory).The mass of the chemicals was measured using a digital weight balance of accuracy up to 0.001%.

Titanium dioxide nanoparticles were prepared by adding 1mol of titanium isopropoxide measured by digital weight balance to 10ml ethanol solution followed by the addition of a few drops of hydrogen peroxide. Ethanol was added to a yellow color solution and the solution was adjusted to 100ml. The solution was kept a constant stirring rate of 360rpm by using hot plate stirrer. The solution was poured to a closed vessel and was heated at 200ºC in an oven for 2 hours so that if any of the particles are still not dissolved, they get dissolved. The solution is heated until the amount of solution starts decreasing. The solution was dried in an oven at 100ºC for 18hours to obtain dry powder as our solution catches fire at high temperatures in the furnace. The solution was completely dried before the calcination process. The dry powder was placed in a furnace using a china dish and was calcinated at 600ºC for 3 hours to obtain white titanium dioxide nanoparticles. The entire process is shown in Figure 4.1.

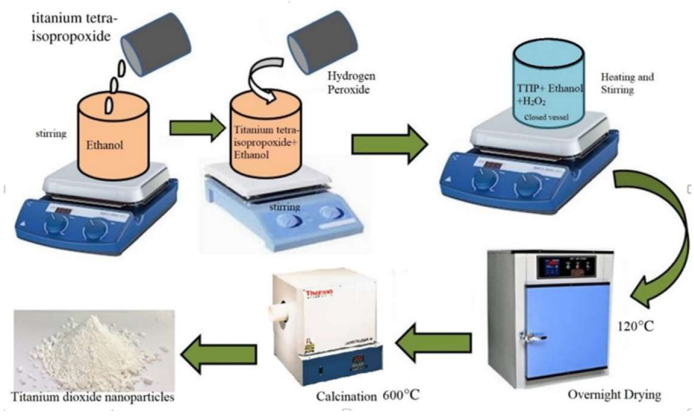

Figure 4.1 Nanoparticles preparation process

4.2 Characterization

4.2.1 X-ray diffraction

It is a technique for the identification of a crystalline material and provides information about the unit cell of the material. It works on the constructive interference between the x-rays and the material sample. This machine consists of three components sample holder, X-ray detector and an X-ray tube. The filament heated in the cathode ray tube produces electrons that are accelerated towards the target using voltage. The electrons are bombarded on the sample. X-ray spectra are produced by the bombarded electrons to dislodge the inner shell electrons of the sample target material. The spectra contain different parts, one with shorter wavelengths while twice the intensity of the other. Each targeted material has specific wavelength characteristics. The X-ray produced is then filtered to convert it into monochromatic radiation, which is then collimated to concentrate the sample. The incident X-ray and the sample results in constructive interference when the interaction satisfy Bragg's law (n λ=2dsinϴ). The diffracted x-rays are then detected, processed and counted. The d spacing obtained from the diffraction peak allows the recognition of the mineral. The particle size is calculated by using the Debye Scherer equation [1]. Philips X-ray diffractometer shown in Figure 4.2 is used for XRD. The angle (2ϴ) was kept in the range of 10^{o} to 80^{o}. The sample was scanned by keeping the generator setting of 35kV and 30A [2]-[4]. It was found out that the nanoparticles are mainly composed of anatase phase of titanium dioxide which was confirmed by the analysis performed on the jade software.

$$D = \frac{k\lambda}{\beta cos\theta} \qquad (1)$$

Where D is the average crystallite size, ϴ is the Bragg angle, λ is the X-ray wavelength, β is the width of the peak in radians due to the finite size of the crystal and k is constant 0.94.

Figure 4.2 Bruker D8 advanced X-ray diffractometer

4.2.2 Scanning Electron Microscopy (SEM) and Energy Dispersive X-ray spectroscopy (EDS)

The Scanning electron microscopy applies a high energy focused beam of electron on the solid sample surface. The specific kinetic energy of the accelerated electrons produces specific signals while dissipating energy at the time of the strike. The signals include backscattered electrons, diffracted electrons backscattered, secondary electrons, visible light, photons, and heat. The secondary electrons are used to generate an SEM image. Photons are used for elemental analysis. Mostly data is measured at a specific location on the sample surface shown by the two-dimensional image. It has a width of 1cm to 5micron with a magnification power of 20X to 30000X and spatial resolution in the range of 50nm to 100nm. The surface morphology, elemental

composition, orientation and crystalline structure of the sample can be obtained by these methods.

The sample needed to be small enough to fit the stage of the specimen and need a special method for increasing electrical conductivity and to stabilize it. Samples are mounted on the stub or specimen holder using adhesives. Conductive materials samples are coated with gold/palladium alloy, gold, iridium, tungsten, graphite, osmium, and chromium. Non conducting samples are tested with coating.

The electron gun with a cathode filled with tungsten filament produces a beam of electrons. 0.2keV to 40keV energy electron beams are focused by condensing lenses to target 0.4nm to 5nm diameter, which then passes through deflecting plates. The final lens deflects the beam in the x-axis or y-axis so that it scans the sample surface. When the electrons strike the sample it loses energy by rapid scattering or absorption in a specific volume known as interaction volume. The interaction volume size depends on electrons' energy of landing, specimen density and the atomic number of specimen. The energy interaction of sample and electron beam results in high energy electrons reflection by scattering elastically, emissions of a secondary electron by emissions. These all will be detected by a special detector. The specimen absorbs current which can be detected by the detector and is used to produce images of the current distribution in the sample. Various kinds of amplifiers can be used to amplify the signal which is displayed in the computer monitor. The computer pixels are synchronized with the beam and the image shows the intensity of the emitted signal in a scanned area. Most of the modern machines collect digital images [5] [6].

Energy-dispersive X-ray spectroscopy (EDS) testing was performed on the sample in conjunction with SEM to determine its composition using Tesan Vega3 scanning electron microscope shown in Figure 4.3. The EDS can provide both quantitative and qualitative composition of the sample.

Figure 4.3 TESAN VEGA3 Scanning electron microscope

4.3 Surfactants

Surfactants can be used to increase the stability of the nanofluid. These surfactants include sodium dodecyl sulfate (SDS), Acetic acid (AA), CTAB, polyvinylpyrrolidone, SDBS. In the current study, CTAB surfactant is used in the amount of 0.1g in the nanofluid. The dispersant reduces the agglomeration of particles by electrostatic repulsion or static hindrance performed by the molecules.

4.4 Preparation of nanofluid

The nanofluid of titanium dioxide nanoparticles with water. The preparation was performed in a two steps method shown in Figure 4.4. The synthesized titanium dioxide nanoparticles were added to deionized water in different concentrations such as 0.05vol%, 0.1 vol%, and 0.2 vol%. The Surfactant was also added to the solution to improve its stability. The solution is sonicated in the probe sonicator for 1 hour so that the particles get well dispersed and the solution remains stable for a longer time. The mass of the nanoparticles, Deionized water, and Cetyl trimethyl ammonium bromide was measured using the electronic sensitive mass balance. The volume concentration of the nanofluid in the nanofluid can be calculated by using the equation.

$$\text{Percent volume concentration } \phi = \left[\frac{\left(\frac{m_p}{\rho_p}\right)}{\left(\frac{m_p}{\rho_p}+\frac{m_b}{\rho_b}\right)}\right] \times 100 \qquad (2)$$

Where m_p is the mass of the titanium dioxide nanoparticles, ρ_p is the density of the TiO_2 nanoparticles, m_b is the mass of the base fluid and ρ_b is the density of the base fluid.

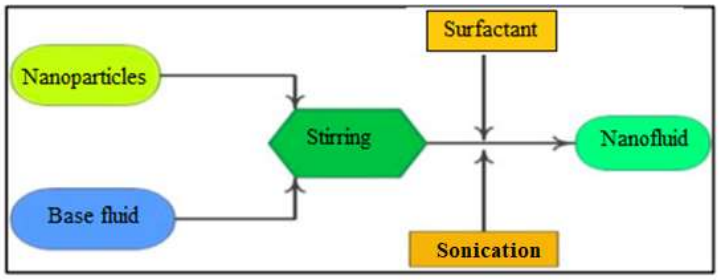

Figure 4.4 Nanofluid fabrication process

4.5 Ultrasound probe sonicator

The QSonica sonicator shown in Figure 4.5 is used for the fabrication of stable nanofluid. The probe sonicator is used for the dispersion of particles in a fluid. It uses high ultrasonic cavitation for breaking up particle agglomeration and produce smaller and uniform particle sizes. Uniform and stable suspensions are mostly required in industrial operations. Probe sonicator usage is highly effective for the preparation of the nanofluid as well as for nanotubes, ink, metal oxides, graphene, etc. Probe sonication can be for improving the stability of the nanofluid. The literature suggests that probe sonication for 1 hour of time interval produces the best nanofluid. The nanofluid containing TiO_2 nanoparticles, water, and cetyl trimethyl ammonium bromide is sonicated for 1 hour at 500watts, frequency of 20 kHz, amplitude 30% and no pulses.

Figure 4.5 QSonica Probe Sonicator

4.6 Stability

It is evaluated for the fluid using +92 UV-Vis spectrophotometer shown in Figure 4.7 and Sedimentation photo capturing. The UV-Vis spectroscopy graphs obtained from performing testing after a few days were compared to check the stability duration of the nanofluid.

4.6.1 UV-Vis Spectroscopy

This measures the attenuation of a light beam after it is reflected from the sample surface or passed through the sample. It can be performed in the range of 1100nm to 190nm or at a specific wavelength only. It is used for the detection of quantitative analysis, qualitative analysis, impurities, functional groups, and nanofluid stability. Most the wavelength from 800nm to 400nm is considered as visible spectrum while from 400 to 180nm is considered as an ultraviolet region.

When the light energy strikes the surface of the sample and its energy difference matches the electronic transition, then the electrons will absorb energy and will get promoted to a higher energy orbital. The spectrometer detects the absorption and plots the absorbance against the wavelength which is known as the absorption spectrum. It follows the Beer's law which states that "The intensity of monochromatic light beam decreases exponentially with increase in concentration of the absorbing substance" and lambert's law which states that "when a light beam is allowed to pass through transparent medium, the rate of decrease of intensity with thickness of the medium is directly proportional to the intensity of light".

Mathematically

Beer's law

$$\mathbf{I = I_o e^{-kc}} \qquad \textbf{(3)}$$

Lambert's law

$$\mathbf{-\ln I = kt + b} \qquad \textbf{(4)}$$

UV-Vis spectrophotometer consists of both deuterium filled with silica and tungsten lamps. One lamp for producing UV light while the second one for visible light. Filters are used to only pass specific wavelengths of the source. The spectrometer which is an assembly of mirrors, lamps, detector, and prisms split energy beam into two parts. One

part of the beam passes through the reference sample while the other part passes through the test sample. Both the reference and test samples were placed in a cuvette made of quartz. The reference sample is basically a fluid in which the test sample is dissolved. The cuvette is designed in a way that the beam of energy can pass through it. When the energy beam passes through the reference and test sample it detects the difference between them. The detector then sends the data to the recorder which is displayed on the screen [7] [8].

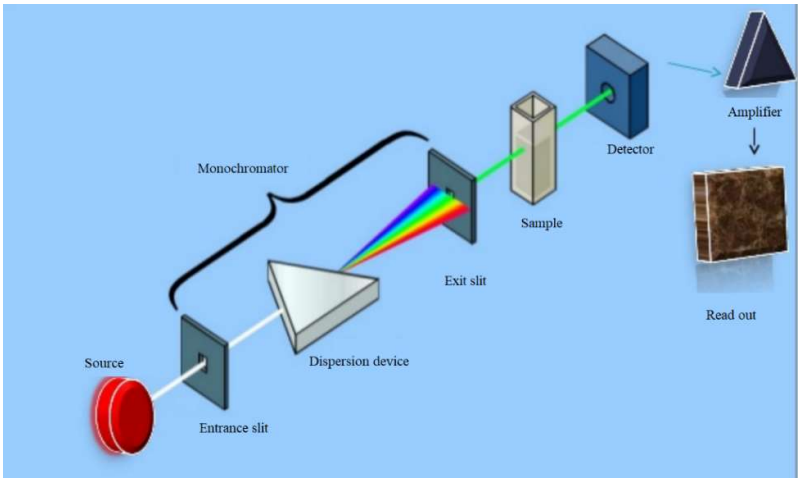

Figure 4.6 Block diagram of UV-Vis spectroscopy [7]

Figure 4.7 T92+ UV-Vis spectrophotometer

4.6.2 Sedimentation Photo capturing

The stability of the nanofluid is also evaluated by using sedimentation images of the nanofluid. The nanofluid images are taken at regular intervals to check the sedimentation of the nanoparticles. The sedimentation of the nanoparticles in the nanofluid increases as the time passes. The nanoparticles settle down to the bottom slowly with the time and when all the nanoparticles settle down to the bottom the nanofluid will no longer be stable. The images of the nanofluid are taken using a cell phone camera.

4.7 Thermo-physical properties of the nanofluid

The determination of the thermophysical properties of the fluid is very important for industrial applications. The thermophysical properties of the nanofluid such as viscosity and thermal conductivity need to be determined to use nanofluid for heat transfer application.

4.7.1 Viscosity of the nanofluid

The viscosity of the nanofluid was determined using a standard programmable viscometer. Brookfield type of viscometer shown in Figure 4.8 is used for the measurement of nanofluid viscosity which uses a spring to measure the torque needed to rotate the spindle. A magnetic rotor lightweight floats in a tube filled with fluid and rotates at a constant speed. The rotor is driven by the viscous force of the fluid. This leads to equilibrium rotor speed which is recorded as fluids viscosity.

Viscometer has a spindle S18 which can measure viscosity from 1cP to 2000cP. The spindle is inserted in the tank containing 16ml of the sample solution and is connected to the viscometer. The viscometer is connected to a computer using cable RS232 and rheocalc software was used for data collection and storage [9]. The variation of the viscosity was determined with the temperature in the range of 30^{o}C to 80^{o}C at a constant rotational speed of the spindle while the variation with a rotational speed which changes the shear rate applied on the nanofluid and particle loadings is determined at a constant temperature of 30^{o}C.

Figure 4.8 Brookfield Viscometer DV2T

4.7.2 Thermal Conductivity

The thermal conductivity of TiO_2/H_2O nanofluid is measured using hot disk TPS 2500s shown in Figure 4.9. Hot disk TPS 2500s can be used to measure the thermal conductivity, thermal diffusivity and specific heat capacity of both solids and liquids. It is factory calibrated. The optimally designed hot plate sensor and simplicity of TPS 2500s make it ideal for measuring the thermal properties of solids, liquids, pastes, powders, and foams. It covers many materials and meets the ISO standard 22007-2. It can measure the thermal conductivity in the range of 0.05 to 1800 W/m-K, thermal diffusivity from 0.1 to 1200 mm^2/s and specific heat capacity up to 5 Mj/m^3-K. The probe of the TPS consists of a sensor which acts as a heater for increasing the temperature as well as a resistance thermometer to record the time-dependent temperature increase of the sensor. The sensor element in the TPS is made of electrically conducting a double spiral-shaped Nickle foil. The two layers of insulation are used to sandwich the nickel foil for mechanical strength, a specific shape, and electrical insulation. A stainless-steel holder is used to hold liquid samples.

The TPS sensor is placed between two pieces of the sample that is also in contact with surfaces. The Nickle foil is used to pass the current through the sample which increases the temperature of the sample. The power and time are adjusted according to materials to be tested. The generated heat is dissipated on both sides of the sensors and the rate

is dependent upon the thermal transport properties of the sample. The thermal properties are calculated based on the temperature increase with time of the sensor [10] [11].

Figure 4.9 Thermal conductivity meter (Hot Disk TPS 2500s)

Summary

This section first discusses all the techniques used for the characterization of nanoparticles such as XRD, SEM, and EDS. Further, the fabrication of the nanofluid along with the apparatuses used for fabrication of the nanofluid is discussed in detail. The apparatuses used for thermal properties such as viscosity and thermal conductivity of the nanofluid are also explained in detail.

References

[1] A.L Patterson, "The Scherrer Formula for X-ray Particle Size Determination," *Phys. Rev.*, vol. 56, pp. 978–982, 1939.

[2] D. Banerjee, "X-Ray Diffraction (XRD)," *www.iitk.ac.in*, 2017. [Online]. Available: https://www.iitk.ac.in/che/pdf/resources/XRD-reading-material.pdf. [Accessed: 01-Mar-2020]

[3] C. M. C. Barbara L Dutrow, "X-ray Diffraction (XRD)," *serc.carleton.edu*, 2020. [Online]. Available: https://serc.carleton.edu/research_education/geochemsheets/techniques/XRD.html. [Accessed: 01-Mar-2020]

[4] P. (University of P. Heiney, "X-ray Powder Diffraction," *www.physics.upenn.edu*, 2019. [Online]. Available: https://www.physics.upenn.edu/~heiney/datasqueeze/technical.html. [Accessed: 01-Mar-2020].

[5] Hayley Anderson, "Scanning Electron Microscope," *www.microscopemaster.com*, 2012. [Online]. Available: https://www.microscopemaster.com/scanning-electron-microscope.html. [Accessed: 01-Mar-2020].

[6] U. of W. Susan Swapp, "Scanning Electron Microscopy (SEM)," *serc.carleton.edu*, 2017. [Online]. Available: https://serc.carleton.edu/research_education/geochemsheets/techniques/SEM.html. [Accessed: 01-Mar-2020].

[7] Frank van Geel, "UV/Vis spectrometry basics - UV/Vis spectrometry basics - Chromedia," *www.chromedia.org*, 2020. [Online]. Available: https://www.chromedia.org/chromedia?waxtrapp=fotjtbEsHiemBpdmBlIEcCAtB&subNav=lnijabEsHiemBpdmBlIEcCAtBN. [Accessed: 01-Mar-2020].

[8] William Reusch, "UV-Visible Spectroscopy," *chemistry.msu.edu*, 2013. [Online]. Available: https://www2.chemistry.msu.edu/faculty/reusch/VirtTxtJml/Spectrpy/UV-Vis/spectrum.htm. [Accessed: 01-Mar-2020].

[9] B. engineering Lab, "BROOKFIELD DV2T Viscometer," *brookfieldengineering.com*. [Online]. Available: https://www.brookfieldengineering.com/-/media/ametekbrookfield/manuals/lab viscometers/dv2t instructions.pdf?la=en. [Accessed: 01-Mar-2020].

[10] A. Ashraf, "Measurement of Thermal Conductivity and Diffusivity of Different Materials by the Transient Plane Source Method Using Hot Disk Thermal Constants Analyzer," *Therm. Conduct. Meas. by Hot Disk Anal.*, 2016. [Accessed: 01-Mar-2020]

[11] Thermtest, "Hot Disk TPS," *thermtest.com*. [Online]. Available: https://thermtest.com/wp-content/pdf/Thermtest-Hot-Disk.pdf. [Accessed: 01-Mar-2020]

Chapter 5

Results and Discussions

The current study demonstrates the synthesis of nanoparticles, characterization of nanoparticles. It further explains the preparation of nanofluid, stability of the nanofluid and thermal properties of the nanofluid.

5.1 Characterization of nanoparticles

The prepared TiO_2 nanoparticles were characterized using XRD, SEM, and EDS. The characterization of the particles is important to be sure that the prepared particles are according to the requirement of our objectives. The XRD characterization is important because it determines if particles are in pure form or impure form. It also determines the phase of the particles. The SEM characterization helps in determining the shape of the particles. The EDS results shows all the elements present in the prepared particles and helps in the determination of the purity of the sample.

5.1.1 X-Ray diffraction

The purity, phase and crystallite size of the particles can be evaluated using X-ray Diffractometer. The powdered sample was placed in the sample holder. The sample holder is then placed in the diffractometer where the x-rays are passed through the sample. The pattern obtained from XRD was analyzed using jade 6.5, which confirmed the formation of both anatase phase and the rutile phase of the TiO_2 nanoparticles. Figure 5.1 shows the XRD pattern of TiO_2 nanoparticles. The peak (101) at Θ=25.25° and Θ=48° confirms the formation of the anatase phase (pdf# 71-1166) while the peak (110) at Θ=27.42° shows the formation of the rutile phase (pdf#86-0147). These peaks were well matched with the literature [1]. The average crystallite size calculated is approximately 23±3 nm calculated by the Debye Scherer formula.

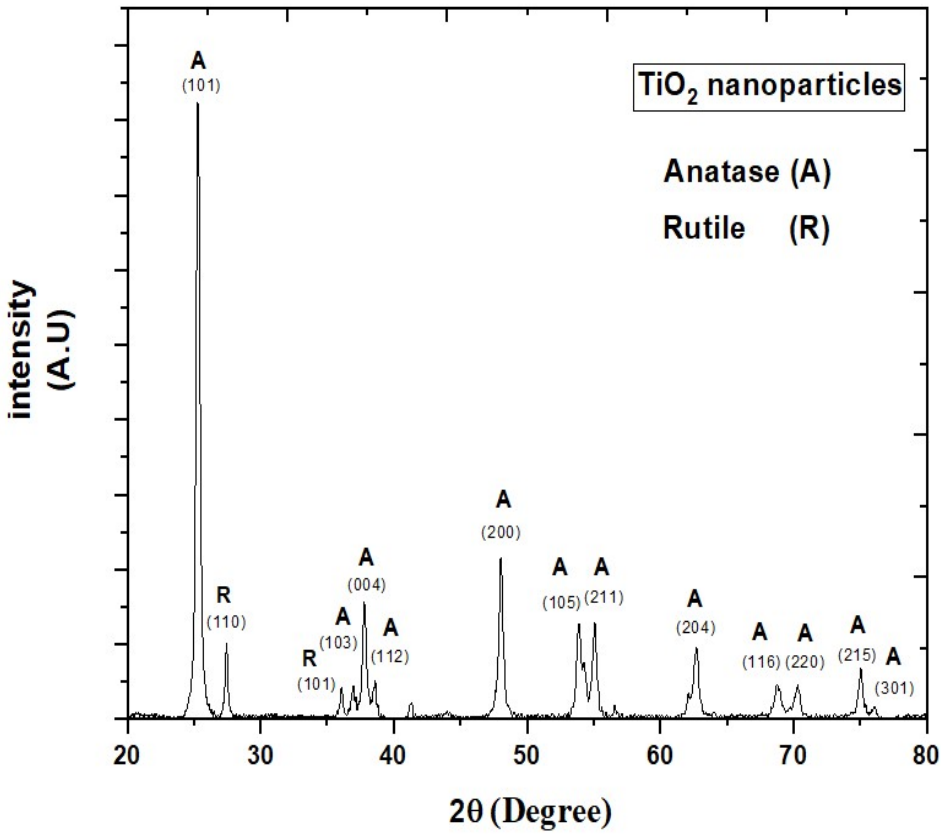

Figure 5.1 XRD Pattern of titanium dioxide nanoparticles

5.1.2 Scanning Electron Microscopy

TESAN VEGA3 Scanning Electron Microscope was used to analyze the morphology and size of titanium dioxide nanoparticles. Micrographs were obtained at a desired accelerated voltage to obtain the best possible resolution by a secondary electron imaging device. It was found that the nanoparticles are mostly in a spherical shape. Figure 5.2 shows the SEM results of the sample that confirms that the particles are well agglomerated. The diameter of the smallest particles is found to be below 50nm while the average size of the particles is above 50nm. The determination of the average diameter is difficult as most of the particles are well agglomerated.

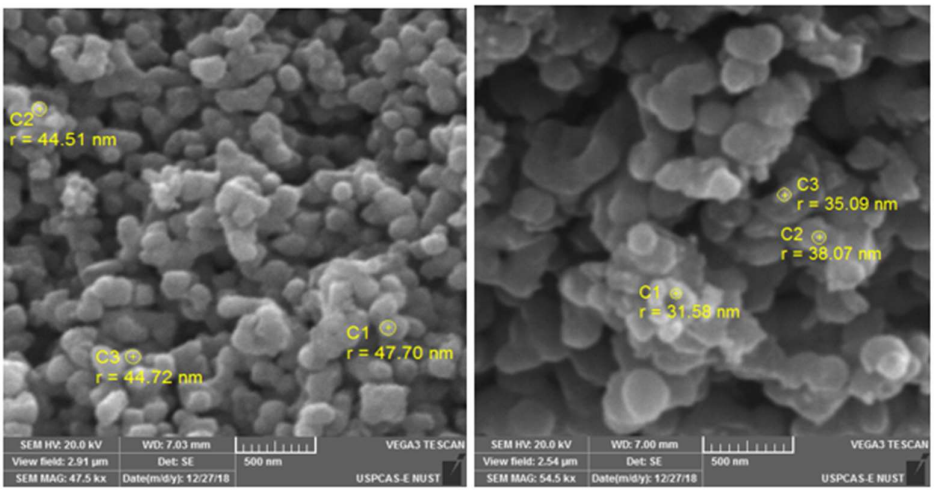

Figure 5.2 SEM image of titanium dioxide nanoparticles

5.1.3 Energy-dispersive X-ray spectroscopy (EDS)

EDS testing was performed on the TiO_2 sample in conjunction with SEM to determine its elemental composition. The EDS provides both quantitative and qualitative composition of the sample. The EDS results shown in Figure 5.3 show that the sample contains titanium (Ti), oxygen (O_2), carbon (C) and some amount of aurum (Au) were found. Au was found due to gold electroplating performed during the preparation of the sample for SEM and EDS testing.

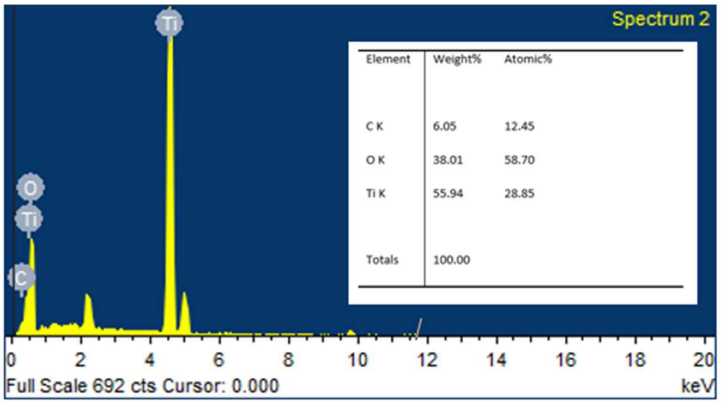

Figure 5.3 EDS pattern of nanoparticles

5.2 Stability evaluation of the nanofluid

The nanofluid containing water, titanium dioxide nanoparticles and CTAB surfactant is prepared by two steps method.

5.2.1 UV-Vis spectroscopy

The stability of TiO_2/H_2O nanofluid with CTAB surfactant and without surfactant are evaluated using UV-Vis spectroscopy. The UV/Vis spectroscopy results in Figure 5.4 show that the stability of the nanofluid without surfactant for the concentration of 0.03vol%. The results show that stability decreases as time passes due to the agglomeration and settling down of the particles. Although it is clear from the graph that after 10 days the peaks are at a lower value compared to the first 10 days but there were still enough particles suspended in the fluid that it can be considered as stable. At day 20 all of the nanoparticles settled down to the bottom of the fluid which gives us the stability TiO_2- H_2O nanofluid. It is clear from the UV-Vis spectroscopy results that the nanofluid was stable for 17 days. Figure 5.5 shows the UV-Vis absorbance spectra of the TiO_2/H_2O nanofluid with CTAB surfactant taken at different intervals of time. The absorbance of the sample containing the surfactant is high for more days compared to the sample without surfactant which shows that the addition of the surfactant signifantly improved the stability of the nanofluid. The stability of the nanofluid is observed to be more than 60 days in case of nanofluid containing surfactant compared to 17 days of stability observed in case of nanofluid without surfactant.

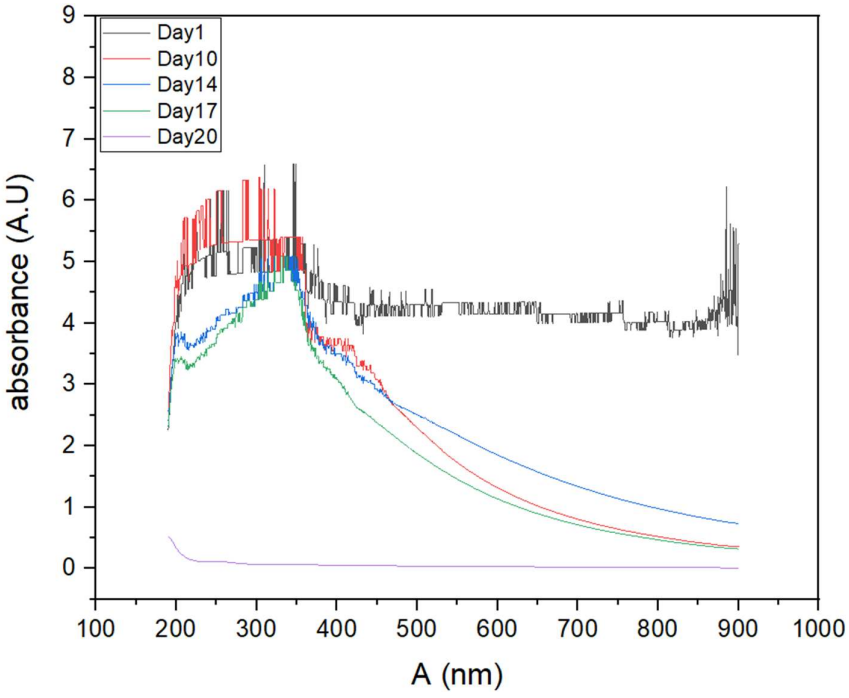

Figure 5.4 UV-Vis spectra of 0.05vol% TiO_2- H_2O nanofluid without surfactant

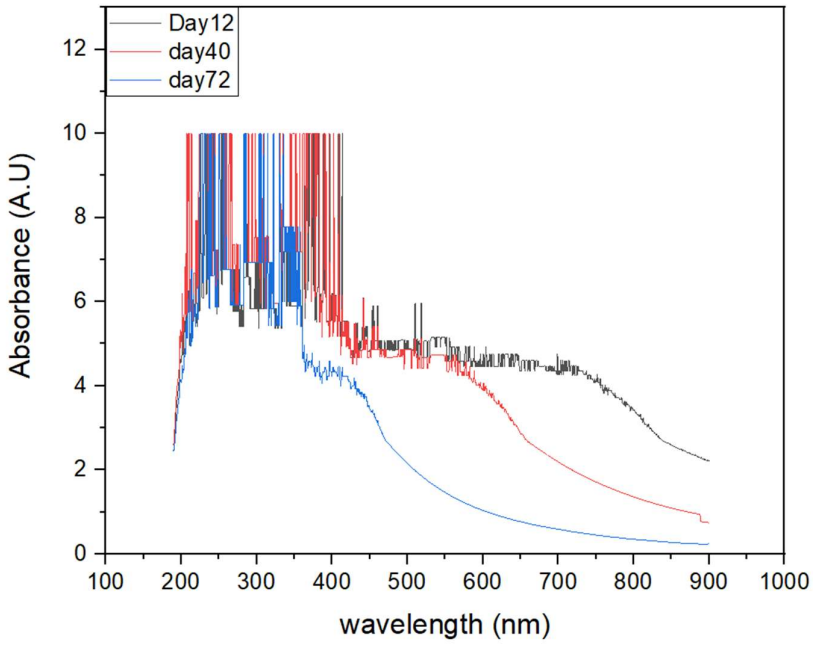

Figure 5.5 UV-Vis spectra of 0.2vol% TiO_2- H_2O nanofluid with CTAB surfactant

5.2.2 Sedimentation Photo capturing

Figure 5.6 shows the sedimentation images of TiO_2-H_2O nanofluid without surfactant taken at different intervals of time. The more the nanoparticles are suspended in the nanofluid the higher will be its stability, and as the particles settle down the nanofluid is no longer stable. It can be seen in the images that as the particles settles down the color of the nanofluid changes and the fluid becomes thinner and when all the particles settles down to the bottom the nanofluid become same as simple water kept in a beaker. The sedimentation images confirm the results obtained from the UV-Vis spectroscopy. It is clear from the image that enough number of nanoparticles are still suspended in the nanofluid till day 17 that it can be considered as stable and after 20 days all the particles.

Figure 5.7 shows the sedimentation image of TiO_2/H_2O nanofluid with surfactant taken at different intervals of time. It can be seen in the images that the nanofluid is stable for more than 60 days which means that the addition of CTAB surfactant improves the stability of the nanofluid significantly.

Figure 5.6 Sedimentation photograph of 0.05vol% TiO_2- H_2O nanofluid without surfactant (a) Before sonication (b) Day1 after sonication (c) Day9 (d) Day 13 (e) Day17 (f) Day 20

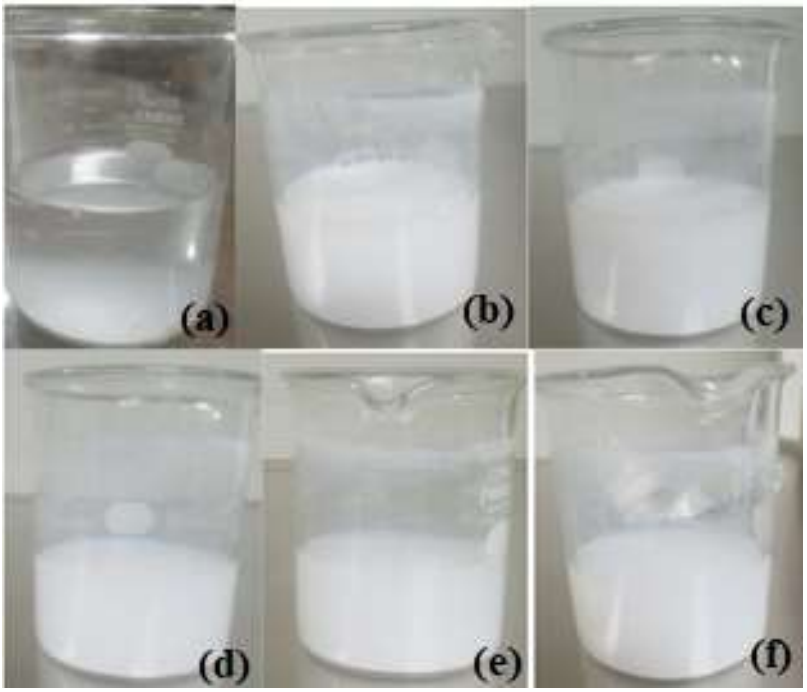

Figure 5.7 Sedimentation photograph of 0.2vol% TiO_2- H_2O of nanofluid with surfactant (a) Before sonication (b) Day1 after sonication (c) Day17 (d) Day 32 (e) Day44 (f) Day 60

5.3 Viscosity of nanofluid

The viscosity of the nanofluid is measured with the DV2T viscometer. Figure 5.8 shows the variation of viscosity with temperature for TiO_2/H_2O nanofluid stabilized using CTAB surfactant at different particle loadings at a shear rate of $100s^{-1}$. The viscosity of the nanofluid is also compared with the conventional fluid. It is observed that the viscosity varies inversely with the temperature of the sample for all concentrations of nanofluid and the base fluid.

Figure 5.9 shows the variation viscosity with the shear rate applied to the sample for TiO_2/H_2O nanofluid stabilized by CTAB surfactant at different particle loadings and fix temperature of 30ºC. It is examined that the viscosity of the nanofluid increases as the shear rate of the nanofluid is raised.

Figure 5.10 shows the variation viscosity with the particle concentration of the sample for TiO_2/H_2O nanofluid stabilized by CTAB surfactant at temperature and shear rate of $100s^{-1}$. The results confirmed that the viscosity of the nanofluid is raised as more particles are loaded into the base fluid.

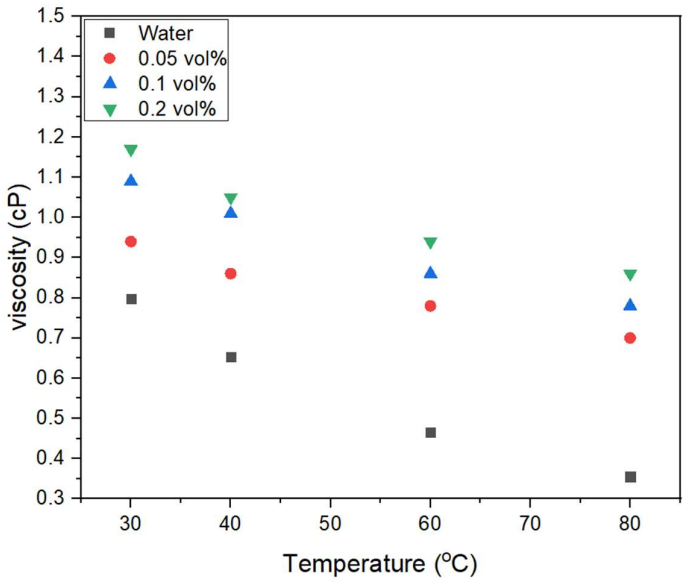

Figure 5.8 Viscosity variation with temperature

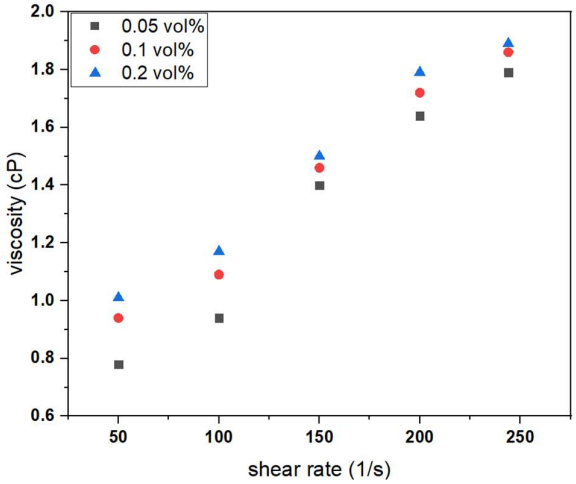

Figure 5.9 Viscosity variation with shear rate

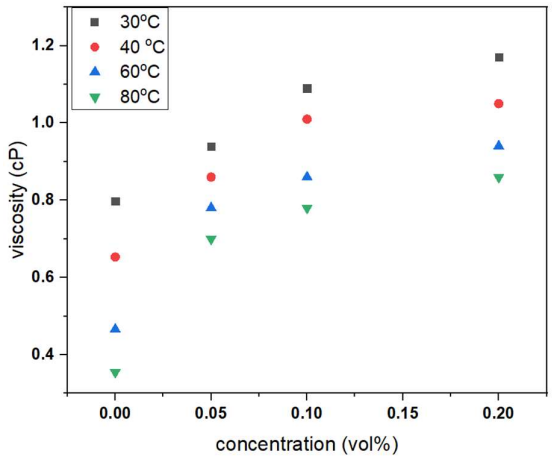

Figure 5.10 Viscosity variation with the concentration of nanoparticles

5.4 Thermal conductivity of nanofluid

It determines the performance and the heat transfer characteristic of the fluid used in an application. The thermal conductivity needs to be enhanced significantly to justify the argument of replacing the conventional fluid with the nanofluid. The thermal conductivity of the nanofluid was measured for different particle loadings at room temperature. The thermal conductivity of the nanofluid was observed to be greater than the thermal conductivity of water. Figure 25 shows that the thermal conductivity of the nanofluid increases as the concentration of the nanoparticles were increased in the sample. The maximum thermal conductivity was obtained for the concentration of 0.2 vol%. Table 1 shows the summary of thermal conductivity observed in different studies.

The thermal conductivity is observed to be increasing with the increase of both particle concentrations and temperature of the sample. In current study the thermal conductivity is observed to be enhanced by 2% to 3% at room temperature which is within the range of different studies performed on the thermal conductivity of the titanium dioxide nanofluid. It is observed that the enhancement in the thermal conductivity increases as the temperature on the sample is increased which can be seen in the table.

Table 5.1 summary of thermal conductivity enhancement in different studies

Author	Base fluid	Temperature °C	Concentration Vol%	Thermal Conductivity enhancement
Oliveira[2]	Water	20-50	0 to 0.1	6.14% at 0.05vol%
Longo [3]	Water	1-40	1 to 6	16%
Najiha [4]	Water	25	0.5, 2,4.5	11.4% at 4.5 vol%
Reddy [5]	EG/ water	30 to 70	0.2 to 1	water 5.01% at 1vol% and EG/water 50:50 14.2% at 1vol%
Azmi [6]	Water	30 to 60	0.5 to 3	26%
Murshed [7]	Water	Room temperature	0.5 to 5	33%
Kim [8]	water/ EG	20	1 to 3	15.40%
Chopker [9]	Water	30	0 to 3	7%
Turgut [10]	Water	13 to 55	0.2 to 3	7.40%

Figure 26 shows the comparison of the experimental values with classical models used for the calculation of thermal conductivity theoretically. The models include Maxwell model, Wasp model, Yu and Choi model, Timofeera model and Murshed model. These models are shown in Table 2. The experimental results were found to be in good agreement with the values calculated from theoretical models.

Table 5.2 Models used for predicting thermal conductivity of nanofluid

Author	Remarks	Model
Maxwell [11]	For spherical particles	$\frac{K_{nf}}{K_f} = \frac{K_p + 2K_f + 2\varphi(K_f - K_p)}{K_p + 2K_f - \varphi(K_f - K_p)}$
Wasp [12]	For spherical particles	$\frac{K_{nf}}{K_f} = \frac{K_p + 2K_f - 2\varphi(K_f - K_p)}{K_p + 2K_f + \varphi(K_f - K_p)}$
Timofeera [13]		$\frac{K_{nf}}{K_f} = 1 + 3\varphi$
Yu and Choi [14]	"β is the ratio of the nano-layer thickness to the original particle radius. Normally, β=0.1 is used to calculate the thermal conductivity of nanofluid"	$\frac{K_{nf}}{K_f} = \frac{K_p + 2K_f + 2\varphi(K_p - K_f)(1+\beta)^3}{K_p + 2K_f - 2\varphi(K_p - K_f)(1+\beta)^3}$
Murshed [7]	$\triangle = (3\varphi - 1)^2 \left(\frac{K_p}{K_f}\right)^2 + (2 - 3\varphi)^2 + 2(2 + 9\varphi + 9\varphi^2)\frac{K_p}{K_f}$	$\frac{K_{nf}}{K_f} = \frac{1}{4}[(3\varphi - 1)\frac{K_p}{K_f} + (2 - 3\varphi)] + \frac{\triangle^{\frac{1}{2}}}{4}$

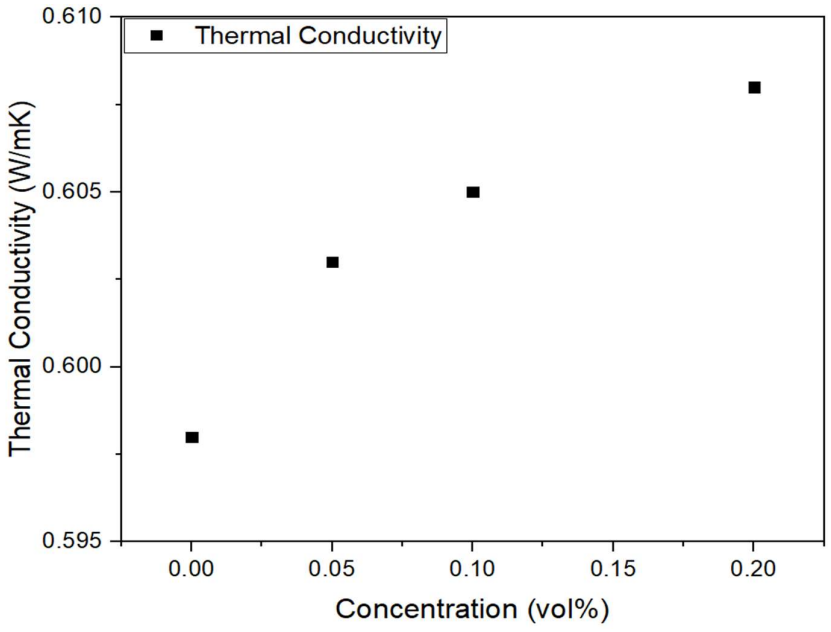

Figure 5.11 Thermal conductivity variation with Concentration of nanoparticles

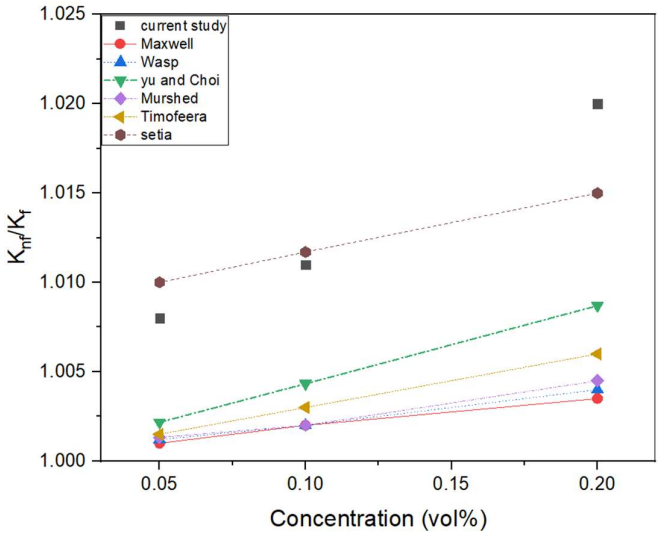

Figure 5.12 Thermal conductivity enhancement

The experimental values were found to be lower than the Oliviera results while higher than all the other models. The measured values were close to Setia results. The highest value of the thermal conductivity for the nanofluid was observed to be 0.2vol% concentration of titanium dioxide nanoparticles.

Summary

In this section, all the results are discussed in detail. In the first part, the nanoparticles characterization results are discussed in detail while in the second part the results related thermal properties are explained. Titanium dioxide nanoparticles preparation were confirmed while the nanofluid was found to be stable for 17 days without surfactant and stable for 2 months with the surfactant addition. The nanofluid were more viscous with higher shear rate and particles loadings while less viscous with higher temperature. Thermal conductivity increased with particles loading.

References

[1] H. Ijadpanah-saravi, M. Safari, and A. Khodadadi-darban, “Synthesis of Titanium Dioxide Nanoparticles for Photocatalytic Degradation of Cyanide in Wastewater,” no. June, 2014.

[2] L. Raquel, A. Christine, A. Silva, N. Oliveira, and E. P. Bandarra, “International Journal of Heat and Mass Transfer Thermophysical properties of TiO_2 -PVA / water nanofluids,” vol. 115, pp. 795–808, 2017.

[3] G. A. Longo and C. Zilio, “Experimental measurement of thermophysical properties of oxide – water nano-fluids down to ice-point,” *Exp. Therm. Fluid Sci.*, vol. 35, no. 7, pp. 1313–1324, 2011.

[4] M. S. Najiha, M. M. Rahman, and K. Kadirgama, *Performance of water-based TiO_2 nanofluid during the minimum quantity lubrication machining of aluminium alloy, AA6061-T6*. Elsevier Ltd, 2016.

[5] M. C. S. Reddy and V. V. Rao, “Experimental studies on thermal conductivity of blends of ethylene glycol-water-based TiO_2 nanofluids ☆,” *Int. Commun. Heat Mass Transf.*, vol. 46, pp. 31–36, 2013.

[6] W. H. Azmi, K. V Sharma, R. Mamat, G. Naja, and M. S. Mohamad, “The enhancement of effective thermal conductivity and effective dynamic viscosity of nano fluids – A review,” vol. 53, pp. 1046–1058, 2016.

[7] S. M. S. Murshed, K. C. Leong, and C. Yang, “Enhanced thermal conductivity of TiO_2 — water based nanofluids,” vol. 44, pp. 367–373, 2005.

[8] S. R. Choi and D. Kim, “Thermal Conductivity of Metal-Oxide Nanofluids : Particle Size Dependence and Effect of,” vol. 129, no. March 2007, 2013.

[9] M. Chopkar, S. Sudarshan, P. K. Das, and I. Manna, “Effect of Particle Size on Thermal Conductivity of Nanofluid,” vol. 39, no. July, 2008.

[10] H. P. S. C. S. S. Tavman, “of Water-Based TiO 2 Nanofluids,” pp. 1213–1226,2009.

[11] J.C. Maxwell, "A Treatise on Electricity and Magnetism", second ed., Clarendon Press, Oxford, UK, 1881.

[12] F.J. Wasp, "Solid–liquid slurry pipeline transportation," Trans. Tech, Berlin,1977".

[13] E. V Timofeeva *et al.*, “Thermal conductivity and particle agglomeration in

alumina nanofluids : Experiment and theory," pp. 28–39, 2007.

[14] W. Yu and S. U. S. Choi, "The role of interfacial layers in the enhanced thermal conductivity of nanofluids : A renovated Hamilton – Crosser model," pp. 355–361, 2004.

Chapter 6

Conclusion and Recommendations

TiO_2 nanoparticles were prepared using a wet chemical method. The nanofluid was prepared by two steps methods. The stability and thermophysical properties of the nanofluid were evaluated for the practical application. The effect of CTAB surfactant on the stability is evaluated and the thermophysical properties were measured at different concentrations and temperatures.

- The preparation of the titanium dioxide is confirmed by X-ray diffraction. The SEM results show the formation of spherical shape and agglomerated nanoparticles. In EDS results titanium (Ti), oxygen (O2) and some amount of aurum (Au) were found in the sample. Au was found due to gold electroplating performed during the preparation of the sample for SEM and EDS testing.
- TiO_2- H_2O nanofluid which is stabilized by CTAB. The stability of the nanofluid was tested by UV-Vis, and sedimentation photo capturing shows that the stability was enhanced significantly by the addition of surfactant. The stability was enhanced from 17 days to more than 60days using a surfactant.
- The nanofluid was found to be more viscous compared to water. The nanofluid was observed to become more viscous with the increase of shear rate and particle loadings while it becomes less viscous with the rise in temperature of the sample. The rise in temperature interacts with the intermolecular forces between the fluid and the particles which leads to lower viscosity value at higher temperatures.
- The thermal conductivity of the nanofluid was observed to be higher than water and was found to be increasing with the particle loadings and the maximum thermal conductivity was found for a sample containing 0.2vol% of titanium dioxide nanoparticles. The more particles present to interact with each other through Brownian motion leads to higher thermal conductivity.

Recommendations

- The nanofluid possesses higher thermal conductivity compared to conventional fluids and therefore has better potential for heat transport in different applications.

The application of the nanofluid will improve heat transfer and therefore will enhance the efficiency of the heat exchangers.

- The application of nanofluid in place of conventional fluid will increase the thermal conductivity of working fluid, which is desirable, but it also increases the viscosity which is not good because it increases the pumping power requirement. At high temperatures the viscosity of the nanofluid decreases so the best application of the nanofluid is at higher temperatures since the thermal conductivity will be high while the viscosity will be low which means the heat transfer will be high at a lower cost of pumping power.
- The current study only focuses on the thermal properties at lower concentrations of the nanoparticles (i.e. 0.05%vol, 0.1%vol, and 0.2 %vol) in the nanofluid. In future studies, the behavior of the nanofluid can be studied at higher concentrations of the nanoparticles. The thermal properties of the nanofluids can also be compared based on different types of nanoparticles.

Chapter 7

Desalination using Hydrogels (ASU Research work)

7.1 Introduction:

The lack of drinkable water is one of the biggest issues that the humans are facing in recent times. More than 70% of the earth's surface is covered by water, 97% of the water remains unavailable to human-kind due to its salt content [1]. The National Academy of Engineer's lists as part of its 14 grand engineering challenges, the challenge of providing access to clean water. By 2025 about 1.2 billion people will reside in water stressed countries [2]. "The production of fresh water from seawater or other contaminated water when seen against all the vast and varied industrial activity of the modern world may seem a small thing. But unless it is provided it could prove to be the nail for lack of which, the whole battle of civilization might be lost, even if we solve the energy supply situation" – Robert Silver (UNESCO prize for science 1968). It is necessary to develop such techniques which will help humans in the production of drinkable water so that in future if needed people will be able to deal with the shortage of drinking water.

Desalination is the removal of minerals from the saline water to make it appropriate for drinking. In the past different methods have been used for the purpose of Desalination. This study deals with the hydrogels that can be used for the purpose of desalination. Hydrogels are the class of materials which can transit from hydrophilic to hydrophobic upon the application of proper stimuli. Thermo-responsive hydrogels such as N-isopropylacrylamide alternate between hydrophobic and hydrophilic at a lower critical Solution temperature of 32ºC. When the hydrogels absorb water, it swells up. The swelling of hydrogels creates Osmotic Pressure across the membrane that forces water out from the feed side of a FO cell through the membrane as shown in fig 7.1. The semi-permeable membrane made of cellulose triacetate was used so that only water passes through it.

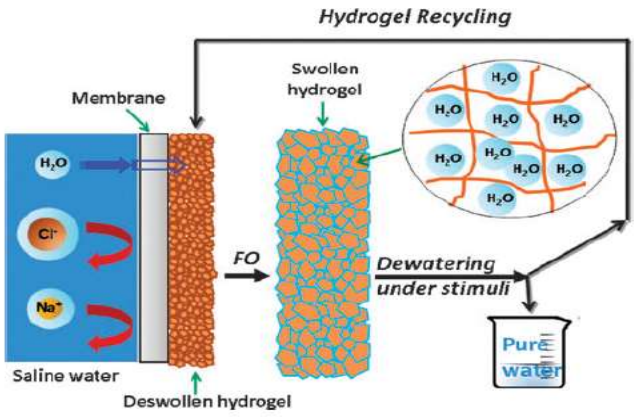

Figure 7.1 Hydrogels Desalination process [3]

7.2 Synthesis of NIPAM hydrogels:

Sodium acrylate dissolved in deionized water to form 16.7 wt% solution. After dissolution 0.057g 0f N-N' methylene bisacrylamide was added to the solution. Polymerization initiated by adding 0.04g of ammonium persulphate into solution at 70ºC. The solution was then kept in a nitrogen filled inert atmosphere overnight. This process is performed for the preparation of NIPAM hydrogel. The setup is shown in fig 7.2.

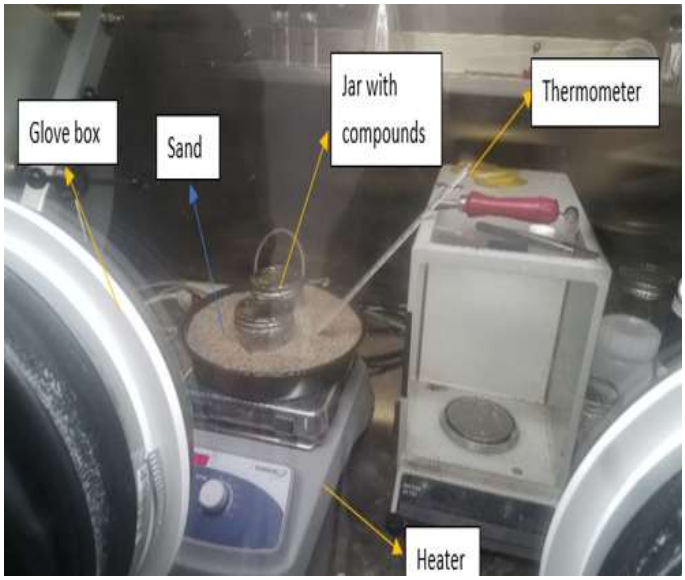

Figure 7.2 Experimental setup for preparation of hydrogels.

7.3 Swelling test of NIPAM:

Swelling testing was performed on the prepared hydrogels to check the its performance. The swelling ratio shows the amount of water absorbed by the hydrogels in a fixed interval of time. The results obtained from the experiment are shown in fig 7.3 which shows that NIPAM prepared in inert atmosphere perform well compared to those prepared in an open atmosphere.

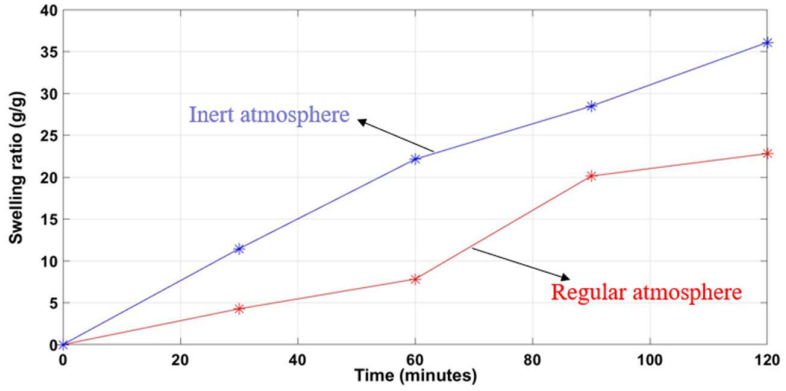

Figure 7.3 Swelling ratio against time NIPAM synthesized in inert and “regular atmosphere".

7.4 Lower critical solution temperature (LCST):

It shows the temperature at which the hydrogel will start dewatering. The experimental setup used for determination of lower critical solution temperature is shown in fig 7.4. The LCST of the NIPAM hydrogel was found to be around 32^{o}C as shown in fig 7.5.

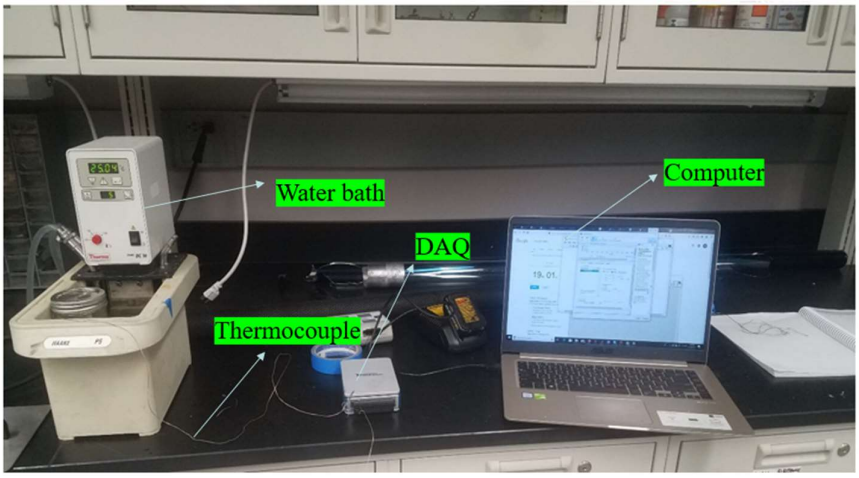

Figure 7.4 Experimental setup for determination of LCST

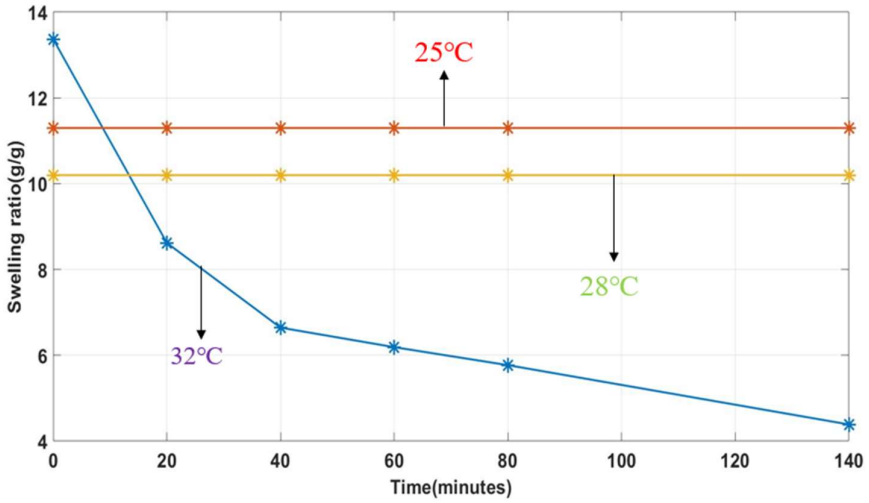

Figure 7.5 LCST result of NIPAM

7.5 Desalination using hydrogels:

Desalination of saline water was performed using NIPAM hydrogels, cellulose triacetate semi-permeable membrane and beaker. The saline water was kept inside the beaker whose mouth is covered with the membrane and the hydrogels were placed above the membrane. The osmatic pressure will be developed due to which the water flows through the membrane to reach the hydrogels. The hydrogels absorb water and swells up. After 48hrs dry NIPAM sample swelled from 0.9103g to 5.0809g. The experimental setup is shown in fig 7.6. The permeation flux was used to determine the performance of the hydrogels as shown in fig 7. The literature suggests that this method desalination can be performed using solar energy as the LCST of hydrogels is low [4].

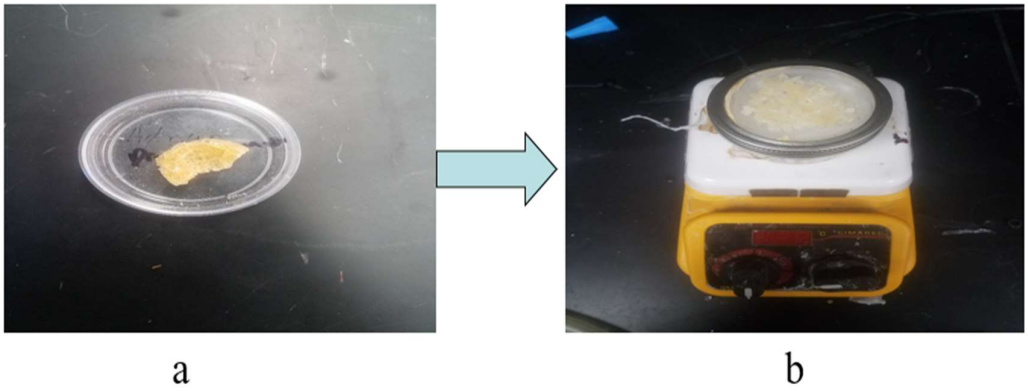

Figure 7.6 (a) Dry hydrogel before absorbing water (b) Hydrogel swells up after absorbing water

The permeation flux comparison with the literature shows consistent results as the permeation decrease with time.

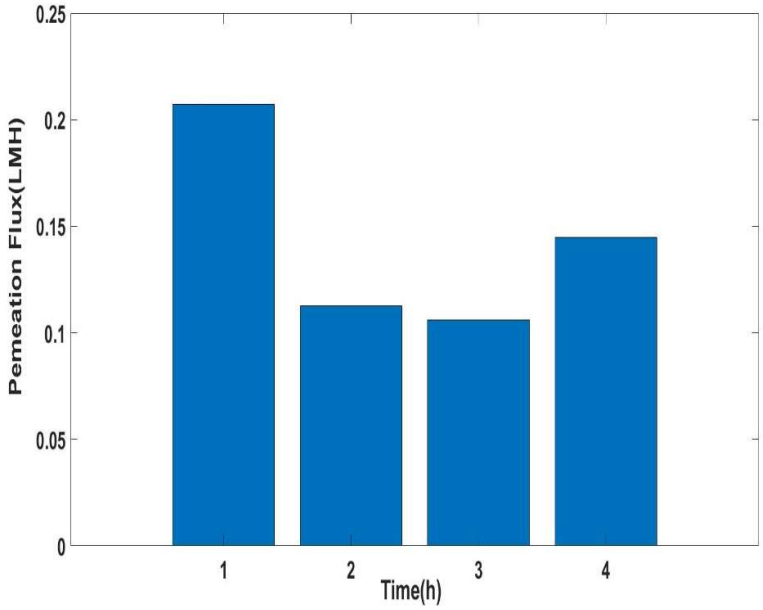

Figure 7.7 Permeation flux over a 4-hour period in current study

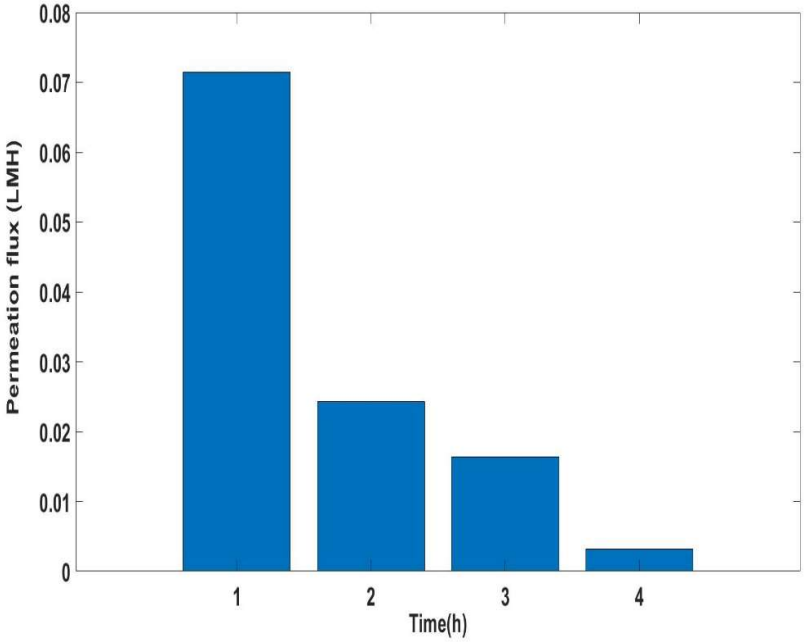

Figure 7.8 Permeation flux over a 4-hour period Comparison with Razmjou et al [5]

Summary:

This work has demonstrated synthesis and characterization of thermo-responsive hydrogels, determination of lower critical solution temperature, and evaluated the performance of thermo-responsive hydrogels as draw agents for FO Desalination.

References:

[1] Charette, Matthew A., and Walter HF Smith. "The volume of Earth's ocean." *Oceanography* 23.2 (2010): 112-114

[2] Ibrahim, G. S., Isloor, A. M., & Yuliwati, E. (2019). A Review: Desalination by Forward Osmosis. In *Current Trends and Future Developments on (Bio-) Membranes* (pp. 199-214). Elsevier.

[3] Li, D., Zhang, X., Yao, J., Simon, G. P., & Wang, H. (2011). Stimuli-responsive polymer hydrogels as a new class of draw agent for forward osmosis desalination. *Chemical Communications*, *47*(6), 1710-1712.

[4] Ibrahim, G. S., Isloor, A. M., & Yuliwati, E. (2019). A Review: Desalination by Forward Osmosis. In *Current Trends and Future Developments on (Bio-) Membranes* (pp. 199-214). Elsevier.

[5] Razmjou, A., Liu, Q., Simon, G. P., & Wang, H. (2013). Bifunctional polymer hydrogel layers as forward osmosis draw agents for continuous production of fresh water using solar energy. *Environmental science & technology*, *47*(22), 13160-13166.

Evaluation of Stability and Rheological Behavior of TiO_2-H_2O Nanofluid

Muhammad Assad Khan[1*], Majid Ali[1], Waqas Ahmad[1]

*Email:engr.assadkhan948@gmail.com

1: US Pakistan center for advanced studies in energy NUST Islamabad Pakistan

Abstract

Nanofluid is the suspension of nanomaterials in the conventional fluid. The nanofluid possesses interesting thermal properties and features due to which it has the potential for different applications. The current study deals with the synthesis of titanium dioxide nanoparticles and fabrication of water-based titanium dioxide nanofluid along with cetyl trimethyl ammonium bromide surfactant using sonication for stability enhancement. The nanoparticles are prepared by the chemical method. The nanoparticles are characterized using the scanning electron microscope, energy-dispersive X-ray spectroscopy, and X-ray diffractometer. Stability is important in the practical application of the nanofluid. Nanofluid stability is evaluated using photo capturing and UV-Vis spectroscopy. The rheological behavior of water-based titanium dioxide nanofluid is evaluated with temperature (30 ^oC, 40 ^oC, 60 ^oC and 80 ^oC), particle loadings (0.01vol%, 0.02vol%, 0.03vol %) and shear rate (50 s^{-1}, 100 s^{-1}, 150s^{-1}, 200 s^{-1}, 245s^{-1}). The characterization confirmed the formation of nanoparticles. The nanofluid is found to be stable for almost 408 hours. The nanofluid viscosity increases as the shear rate and particle loading are increased while it decreases with the rise of temperature. The highest viscosity was observed for 0.03vol% at 245 s^{-1} shear rate and 30 ^oC.

Keywords: Titanium dioxide nanoparticles, nanofluid, viscosity, UV-Vis spectroscopy, CTAB.

1. Introduction

In past researchers have tried to enhance the performance of the heat exchange systems for various applications. The researchers have attempted to lower the size of the heat exchanging systems by improving the heat exchange surfaces with fins etc. and by improving the properties of the heat exchanging fluids to increase its thermal conductivity. The nanotechnology developments have led researchers to prepare different types of nanomaterials which can be suspended in the fluids such as ethylene glycol, engine oil, and water. Choi in 1995 developed a fluid containing nanomaterials suspended in a fluid known as nanofluid, which possessed improved thermal properties compared to conventional fluid and offered stability for a long period of time[1]. Nanofluid possesses better thermal conductivity and therefore has better ability for heat transport in various applications such as electronic devices cooling [2][3], solar heating system[4]–[7], engine cooling system[8]–[13], etc.

Researchers have focused on titanium dioxide because of its good dispensability in solvents, excellent chemical stability, non-toxicity, and its resistance to organic erosions. Titanium dioxide has three main phases brookite, anatase and rutile. Brookite is not stable while the anatase phase possesses better properties compared to the rutile phase of titanium dioxide [14].

In recent past scientists have developed different techniques for the synthesis of different types of nanoparticles. Mahshid et al prepared titanium dioxide nanofluid using hydrolysis and peptization method. They varied the pH value and calcination temperature of the solution during the preparation of nanoparticles. The results showed that as the calcination temperature is lowered size

of the particles also decreases. Anatase phase is formed below 600 ºC while the transformation of phase to rutile takes place above 600 ºC. Smaller size particles are formed in acidic solution while size increases as the pH of the solution raised [15]. Oliveira et al. used the sol-gel method for the preparation of titanium dioxide nanoparticles [16].

The fabrication of nanofluid is not simply nanoparticles addition to the base fluid. It requires special treatment so that the particles do not agglomerate or settle down to the bottom and the particles are well dispersed so that stable nanofluid is produced. The main difficulty faced in the practical application of the nanofluid is the low stability of the nanofluid. The stability of the nanofluid can be enhanced by ultra-sonication, the surfactant addition or their combination. The pH of the solution maintained at a certain value can also improve the stability but then the application of the nanofluid will be restricted [17].

The most commonly used surfactants for stability enhancement are oleic acid (OA), sodium dodecyl sulfate (SDS), cetyl trimethyl ammonium bromide (CTAB), polyvinyl alcohol (PVA), polyvinylpyrrolidone (PVP), sodium dodecyl-benzene sulfonate (SDBS) and acetic acid (AA). The surfactant reduces the agglomeration of particles by electrostatic repulsion or static hindrance performed by the molecules. Das et al. prepared water-based nanofluid along with different surfactants such as SDS, CTAB, acetic acid, and SDBS. They evaluated the stability of the nanofluid using zeta potential and found that the nanofluid with CTAB and SDS were stable for more than 24 hours. The nanofluid having a CTAB surfactant showed better stability than nanofluid containing other surfactants [18]. Ghadimi et al. fabricated water-based nanofluid with SDS surfactant. According to their results, the nanofluid prepared using 3-hour bath sonication showed better stability compared to nanofluid prepared using 15minute horn sonication. The nanofluid was observed to be stable for more than one year [19].

The viscosity is an important property since it provides information about the pumping power requirement and pressure drop in the system. The viscosity of the nanofluid depends on particle loading, temperature, particle size, particle shape, and shear rate. Turgut et al. fabricated nanofluid containing water and TiO_2 and measured its viscosity in the range of 15 ºC to 55 ºC and 0.2vol% to 3vol%. They concluded that the nanofluid becomes more viscous as the particle loadings are raised and less viscous as the temperature of the sample is raised [20]. Das et al. experimental results confirmed the direct relation of viscosity with particle loading and shear rate while inverse relation with the temperature of the sample [21][22]. Teng et al. found that by raising the temperature from 10ºC to 40ºC for TiO_2 nanofluid at 0.5 wt% the increase of 8.2% to 16% was observed in relative viscosity [23].

In this article, titanium dioxide nanoparticles are prepared using the wet chemical method. The prepared nanoparticles are characterized by energy-dispersive X-ray spectroscopy, scanning electron microscopy, and X-ray diffraction. The nanofluid is fabricated using titanium dioxide nanoparticles, water, and cetyl trimethyl ammonium bromide by the two-step method. The stability of the nanofluid is evaluated using a photo capturing of sedimentation and UV-Vis spectroscopy. The nanofluid viscosity is measured using Brookfield viscometer and its variation is studied for different temperatures, shear rate, and particle loading.

2. Experimental Section

2.1 Preparation and characterization of nanoparticles

Titanium dioxide nanoparticles were prepared using titanium tetra isopropoxide (sigma Aldrich 97%), ethanol (Merck 99%) and hydrogen peroxide (BDH laboratory 35%). 1mol of titanium isopropoxide was added to 1mol ethanol along with few drops of hydrogen peroxide. The solution was adjusted to 100ml using ethanol. The solution was kept at a stirring rate of 400rpm.

The solution was heated at 200 ºC along with stirring at 200rpm. The solution was heated until the solution starts decreasing and a small amount of a highly viscous solution is left. The solution was dried in an oven at 100ºC for 18hours. The solution was completely dried before the calcination process. The powder kept in china dish was placed in the furnace for 3 hours at 600 ºC for the calcination process. TiO_2 particles were obtained after the calcination process.

The phase, crystallite size, and purity of the particles were measured using Bruker D8 advanced x-ray diffractometer. The sample was studied for angle (2Θ) kept in the range of 10 º to 80 º. The sample is kept in the sample holder and is exposed to the x-ray beam. The X-rays are diffracted by the crystals which are detected and map the lattice pattern, which enables us to analyses the shape obtained from the diffracted x-rays. The particle crystallite size is calculated using Debye-Scherer's equation [24].

$$p = \frac{C\lambda_x}{\beta cos\theta} \qquad (1)$$

where λ_x is X-ray radiation wavelength (Cu kα=0.15406nm), p is crystallite size, C is equal to 0.94, Θ is the angle of diffraction, and β is the width of line at half maximum height for peaks. The elemental composition and surface morphology of the nanoparticles are evaluated using TESAN VEGA3 Scanning Electron Microscope. The sample was prepared using the aurum coating.

2.2 Preparation of nanofluid

The preparation of stable nanofluid requires special treatment. The stability can be improved by using sonicator, surfactant, pH value or combination of all these. The behavior of nanofluid is studied at lower concentrations only such as at 0.01vol%, 0.02vol% and 0.03vol% concentration of nanoparticles added to distilled water along with 0.1g CTAB surfactant and the mixture is sonicated for 1 hour using probe sonicator for the mixing and suspending the particles in the fluid. The surfactant is used during the fabrication process to lower the rate of agglomeration in the nanofluid which results in the formation of stable nanofluid. The mass of nanoparticles and surfactant is measured using the digital balance. The particle loadings in volume percentage can be calculated using the equation.

$$\phi = \left[\frac{(\frac{m_n}{\rho_n})}{\left(\frac{m_n}{\rho_n} + \frac{m_{nf}}{\rho_{nf}}\right)}\right] \times 100 \qquad (2)$$

where ρ_n is TiO_2 nanoparticles density, m_n is the mass of the titanium dioxide nanoparticles, m_{nf} is the mass of the fluid and ρ_{fl} is the density of the fluid.

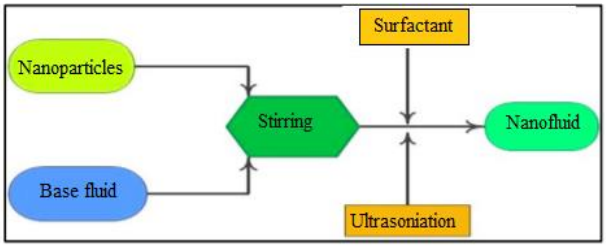

Figure 1 nanofluid preparation process

2.3 Nanofluid stability

The stability of the nanofluid can be observed using photo capturing, UV-Vis spectroscopy and zeta potential. In this study, the stability of water-based titanium dioxide nanofluid is measured using photo capturing and UV-Vis spectroscopy. The images can show the settling down of the particles with time while in UV-Vis the light ray is passed through the sample and standard fluid whose results are compared and we get the value of the difference between their absorbance. The more the particles are suspended in the fluid the higher will be the value of absorbance and the more stable will be the nanofluid.

2.4 Viscosity of nanofluid

The viscosity of titanium dioxide nanofluid for particle loading concentration of 0.01vol%, 0.02vol% and 0.03vol% along with 0.1g CTAB is measured using Brookfield viscometer DV2T. Viscosity is important to be known for the practical application of the nanofluid. Brookfield viscometer DV2T uses a spring to measure the torque needed to rotate the spindle. A magnetic rotor lightweight floats in a tube filled with fluid and rotates at a constant speed. The rotor is driven by the viscous force of the fluid. This leads to equilibrium rotor speed which is recorded as fluids viscosity. A spindle (S18, having a range of measuring viscosity from 1 cP to 2000 cP) is

attached to the viscometer and is inserted in the tank containing 16ml of the sample solution.
The viscosity variation with temperature is measured at temperatures of 30 ºC, 40 ºC, 60 ºC and 80 ºC for all concentrations 0.01vol%, 0.02vol% and 0.03vol% at a shear rate of $100s^{-1}$. The nanofluid behavior for all concentration is also inspected at different shear rate of $50s^{-1}$, $100s^{-1}$, $150s^{-1}$, $200s^{-1}$, $245s^{-1}$ and constant temperature of 30 ºC.

Table 1 particles amount in nanofluid fabrication

Concentration (vol%)	Water(ml) (±0.1ml)	Mass(g) (±0.001g)
0.01	70	0.0264
0.02	70	0.0528
0.03	70	0.0792

3. Results and discussions

3.1 X-ray diffraction

The XRD testing is used for the determination of purity, crystallite size and phase of the particles. The pattern obtained for XRD testing is shown in Figure 4. The (101) peaks show the formation of the anatase phase of TiO_2 (Pdf#1166), well-matched with the literature [25]. The results confirm that the pure anatase phase of titanium dioxide nanoparticles is synthesized as only the peaks of the anatase phase are present in the pattern. The crystallite size calculated by Scherer's equation is around 24+0.3nm.

3.2 Scanning electron microscopy and energy-dispersive x-ray spectroscopy

The SEM and EDS testing were performed for the inspection of surface morphology, the particle diameter, and the elemental composition of the particles. Figure 2 is the SEM images of TiO_2 nanoparticles which shows that spherical shape titanium dioxide nanoparticles are formed. It can also be observed the nanoparticles are well agglomerated with each other and the average diameter of the particles is around 50nm.

The EDS results shown in Figure 3 confirms the presence of only titanium, oxygen in the sample. Although a small amount of aurum is also detected this is because aurum is used during sample preparation for SEM and EDS testing.

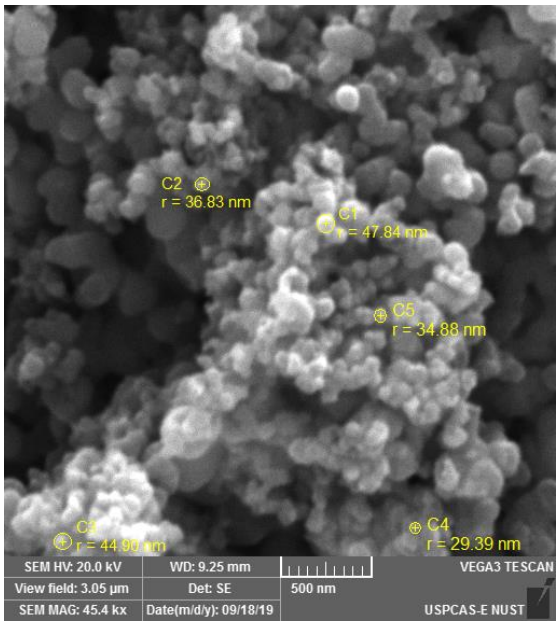

Figure 2 SEM image of TiO_2 nanoparticles

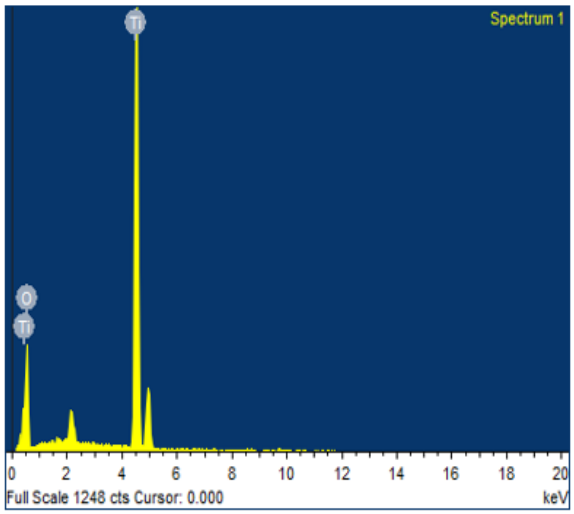

Figure 3 EDS spectra of TiO_2 nanoparticles

3.3 Stability of nanofluid

The fabrication of stable nanofluid is important for practical application. Figure 5 shows the UV-Vis spectroscopy result of nanofluid. According to the results, the nanofluid is stable for almost 408 hours. The more the nanoparticles are suspended in the nanofluid the higher will be the absorbance and hence the more stable will be the nanofluid. It can be seen in the image that the absorbance of the nanofluid is at high value till day 17 which shows that the nanofluid is stable for 17 days. The absorbance decreases with time rapidly and it becomes close to zero after 20 days

which shows that all the particles which were suspended have now settled down to the bottom of the fluid and the fluid is no longer stable. UV-Vis spectroscopy technique for stability evaluation is used by Jiang et al. [26].
The sedimentation photo capturing technique for stability evaluation is also used by Fedele et al. and they found that the TiO_2 based nanofluid was stable for 5 days [27]. Figure 6 shows the photo capturing of the nanofluid on different days. It can be observed in the images that the nanofluid contains enough amount of suspended particles till day17 that it can be considered stable which confirms the UV-Vis results while at day 20 all the particles have settled down to the bottom of fluid.

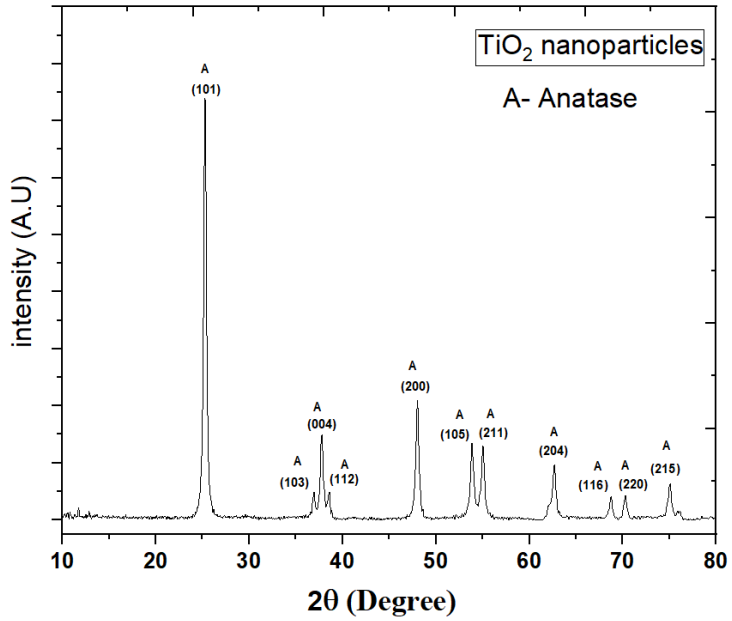

Figure 4 XRD pattern of TiO_2 nanoparticle

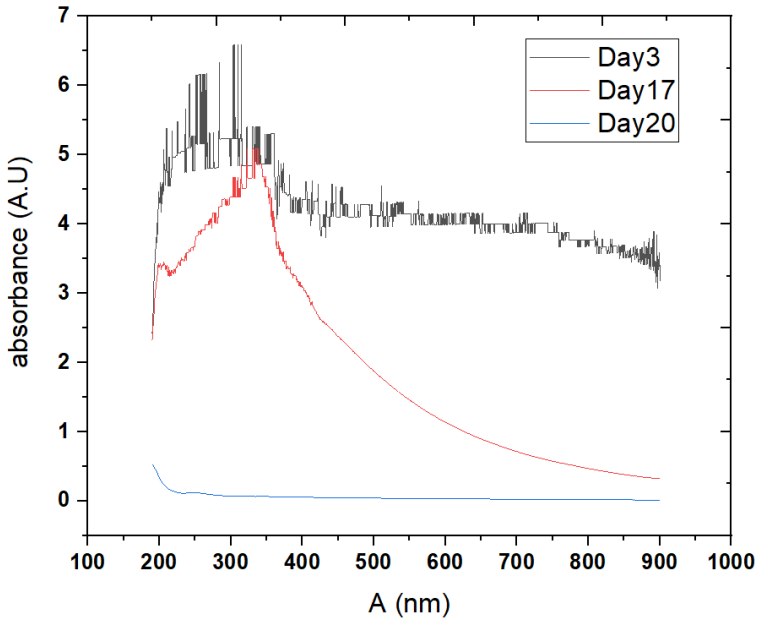

Figure 5 UV-Vis absorbance spectra of TiO_2-water nanofluid sample

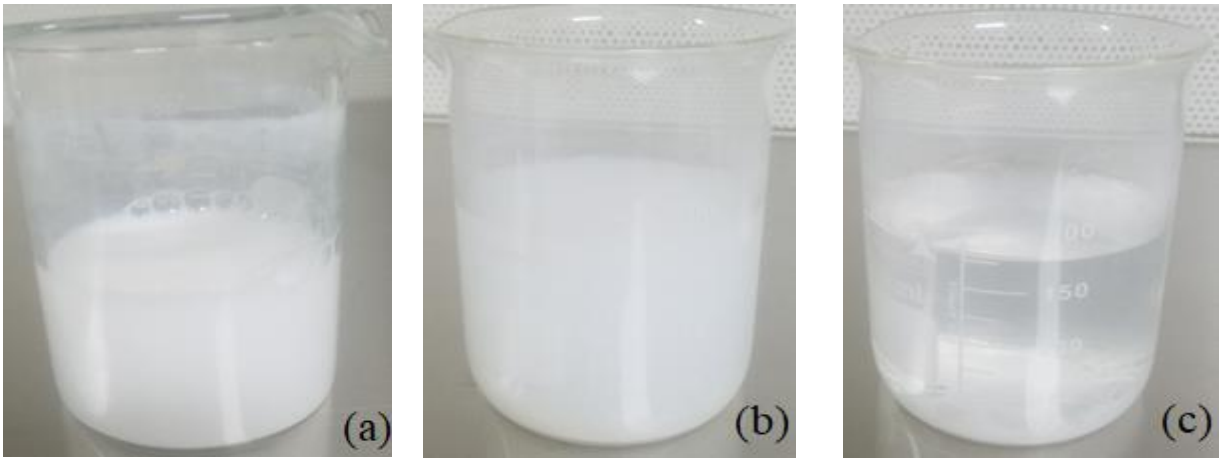

Figure 6 Nanofluid images (a) Day1 (b) Day 17 (c) Day20

3.4 Viscosity of nanofluid

The determination of viscosity is important because it determines the pumping power requirement for the fluid. The viscosity of the nanofluid is expected to be higher than that of the base fluid and therefore can result in more power requirement and in some cases may even decrease the rate of heat transfer, therefore its determination is necessary for practical applications of the nanofluid. The results are shown in Figure 9. According to the results, the viscosity of the nanofluid decreases as the temperature of the sample is raised for all concentrations of the nanofluid. Researchers have observed a similar trend in the viscosity of nanofluid [18], [21].

The variation of viscosity is also evaluated with the number of particle loadings and is represented in Figure 7. The shear rate is kept constant at $100s^{-1}$. The results show that the viscosity of the nanofluid increases with the number of particle loadings at a constant shear rate. Das et al. observed a similar trend in the viscosity of nanofluid [21]. The Utomo et al. experimental results for lower concentration up to 0.03vol% show that the enhancement is observed to be 120% compared to 140% enhancement in the current study which is higher due to the presence of 0.1g of CTAB surfactant [28].

The shear rate applied to the sample also changes the viscosity of the sample. The variation of viscosity with the shear rate is represented in Figure 8. It is observed that the nanofluid viscosity increases with the shear rate of the sample at a constant temperature of 30 °C.

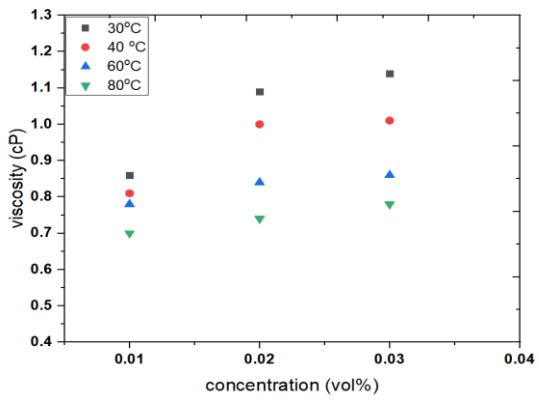

Figure 7 Viscosity variation with concentration at a shear rate of 100 s^{-1}

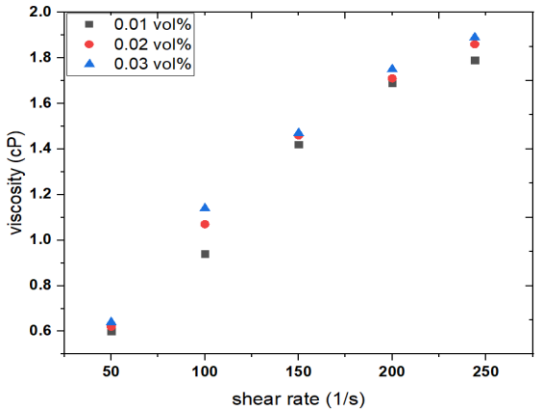

Figure 8 Viscosity variation with a shear rate at 30 °C.

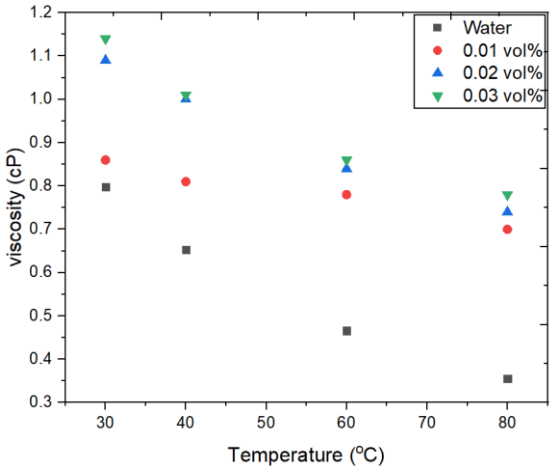

Figure 9 Viscosity variation with the temperature at a shear rate of 100 s^{-1}

Conclusion

In the current study, titanium dioxide nanoparticles were prepared using the wet chemical method. The XRD, SEM and EDS characterization confirmed the formation of spherical shape anatase phase titanium dioxide nanoparticles. The stability of the nanofluid is found to be around 408 hours confirmed by the results of both UV-Vis spectroscopy and sedimentation photo capturing which is good compared to many of the recently published literature. The viscosity of the nanofluid is found to be increasing with particle loadings and shear rate while it decreases as the temperature of the sample is raised. The highest viscosity is found for the concentration of 0.03vol% at a shear rate of 245s^{-1} and a temperature of 30 °C.

References

[1] S. U. S. Choi and J. A. Eastman, "ENHANCING THERMAL CONDUCTIVITY OF FLUIDS WITH NANOPARTICLES *," 1995.

[2] A. Ijam and R. Saidur, "Nanofluid as a coolant for electronic devices (cooling of electronic devices)," *Appl. Therm. Eng.*, vol. 32, pp. 76–82, 2012.

[3] A. M. Siddiqui, W. Arshad, H. M. Ali, M. Ali, and M. A. Nasir, "Evaluation of nanofluids performance for a simulated microprocessor," *Therm. Sci.*, vol. 21, no. 5, pp. 2227–2236, 2017.

[4] T. Youse, F. Veysi, E. Shojaeizadeh, and S. Zinadini, "An experimental investigation on the effect of Al_2O_3- H_2O nanofluid on the efficiency of flat-plate solar collectors," vol. 39, pp. 293–298, 2012.

[5] A. Kasaeian, A. T. Eshghi, and M. Sameti, "A review on the applications of nanofluids in solar energy systems," *Renew. Sustain. Energy Rev.*, vol. 43, pp. 584–598, 2015.

[6] R. Saidur, T. C. Meng, Z. Said, M. Hasanuzzaman, and A. Kamyar, "International Journal of Heat and Mass Transfer Evaluation of the effect of nanofluid-based absorbers on a direct solar collector," *Int. J. Heat Mass Transf.*, vol. 55, no. 21–22, pp. 5899–5907, 2012.

[7] Z. Said *et al.*, "Performance enhancement of a Flat Plate Solar collector using TiO_2 nanofluid and Polyethylene Glycol dispersant," *J. Clean. Prod.*, 2015.

[8] N. A. Che Sidik, M. N. A. Witri Mohd Yazid, and R. Mamat, "Recent advancement of nanofluids in engine cooling system," *Renew. Sustain. Energy Rev.*, vol. 75, no. October 2016, pp. 137–144, 2017.

[9] H. M. Ali, M. D. Azhar, M. Saleem, Q. S. Saeed, and A. Saeed, "Heat transfer enhancement of car radiator using aqua-based magnesium oxide nanofluids," *Therm. Sci.*, vol. 19, no. 6, pp. 2039–2048, 2015.

[10] H. M. Nieh, T. P. Teng, and C. C. Yu, "Enhanced heat dissipation of a radiator

using oxide nano-coolant," *Int. J. Therm. Sci.*, vol. 77, pp. 252–261, 2014.
[11] S. A. Ahmed, M. Ozkaymak, A. Sözen, T. Menlik, and A. Fahed, "Improving car radiator performance by using TiO_2-water nanofluid," *Eng. Sci. Technol. an Int. J.*, vol. 21, no. 5, pp. 996–1005, 2018.
[12] H. M. Ali, M. U. Sajid, and A. Arshad, "Heat Transfer Applications of TiO_2 Nanofluids," *Appl. Titan. Dioxide*, 2017.
[13] K. Y. Leong, R. Saidur, S. N. Kazi, and A. H. Mamun, "Performance investigation of an automotive car radiator operated with nano fluid-based coolants (nanofluid as a coolant in a radiator)," *Appl. Therm. Eng.*, vol. 30, no. 17–18, pp. 2685–2692, 2010.
[14] N. Kaewgabkam, N. Jaitanong, and S. Narksitipan, "Preparation and Characterization of Cement-TiO_2 Composites," vol. 804, pp. 133–136, 2015.
[15] S. Mahata, S. S. Mahato, M. M. Nandi, and B. Mondal, "Synthesis of TiO2nanoparticles by hydrolysis and peptization of titanium isopropoxide solution," *AIP Conf. Proc.*, vol. 1461, no. 1, pp. 225–228, 2011.
[16] L. Raquel, A. Christine, A. Silva, N. Oliveira, and E. P. Bandarra, "International Journal of Heat and Mass Transfer Thermophysical properties of TiO_2 -PVA / water nanofluids," vol. 115, pp. 795–808, 2017.
[17] M. Vakili, A. Mohebbi, and H. Hashemipour, "Experimental study on convective heat transfer of TiO_2 nanofluids," *Heat Mass Transf. und Stoffuebertragung*, vol. 49, no. 8, pp. 1159–1165, 2013.
[18] P. K. Das, A. K. Mallik, R. Ganguly, and A. K. Santra, "Stability and thermophysical measurements of TiO_2 (anatase) nanofluids with different surfactants," *J. Mol. Liq.*, vol. 254, pp. 98–107, 2018.
[19] A. Ghadimi and I. H. Metselaar, "The influence of surfactant and ultrasonic processing on the improvement of stability, thermal conductivity and viscosity of titania nanofluid," *Exp. Therm. Fluid Sci.*, vol. 51, pp. 1–9, 2013.
[20] H. P. S. C. S. S. Tavman, "of Water-Based TiO 2 Nanofluids," pp. 1213–1226, 2009.
[21] P. K. Das, A. K. Mallik, R. Ganguly, and A. K. Santra, "Synthesis and characterization of TiO_2-water nanofluids with different surfactants," *Int. Commun. Heat Mass Transf.*, vol. 75, pp. 341–348, 2016.
[22] S. K. Das, S. U. S. Choi, and H. E. Patel, "Heat transfer in nanofluids - A review," *Heat Transf. Eng.*, vol. 27, no. 10, pp. 3–19, 2006.
[23] T. P. Teng, Y. H. Hung, C. S. Jwo, C. C. Chen, and L. Y. Jeng, "Pressure drop of TiO_2 nanofluid in circular pipes," *Particuology*, vol. 9, no. 5, pp. 486–491, 2011.
[24] P. S. Determination, "No Title," vol. 56, pp. 978–982, 1939.
[25] P. Srinivasu, S. P. Singh, A. Islam, and L. Han, "Novel Approach for the Synthesis of Nanocrystalline Anatase Titania and Their Photovoltaic Application," vol. 2011, 2011.
[26] L. Jiang, L. Gao, and J. Sun, "Production of aqueous colloidal dispersions of carbon nanotubes," vol. 260, pp. 89–94, 2003.
[27] L. Fedele, L. Colla, S. Bobbo, S. Barison, and F. Agresti, "Experimental stability analysis of different water-based nanofluids," pp. 1–8, 2011.
[28] A. T. Utomo, H. Poth, P. T. Robbins, and A. W. Pacek, "International Journal of Heat and Mass Transfer Experimental and theoretical studies of thermal conductivity, viscosity and heat transfer coefficient of titania and alumina nanofluids," *Int. J. Heat Mass Transf.*, vol. 55, no. 25–26, pp. 7772–7781, 2012.